CHEMICAL, MATHEMATICAL AND PHYSICAL SCIENCES DIVISION

CMPSD-1

A STUDY ON THE COMBUSTION CHARACTERISTICS OF EMULSIFIED WATER BLEND IN DIESEL FUEL OIL IN INTERNAL AND EXTERNAL COMBUSTION ENGINES

Kristian G. Basario, Felipe Ronald Argamosa and Neneth Graza

Technological University of the Philippines, Manila

The Philippine government now is facing a tremendous challenge due to the continued rise of petroleum fuel cost. Concerned government agencies are joining hand in hand to find alternative solutions to this energy challenge. In fact, they already have conducted several summits and conferences that directly addressed this energy as well as environmental concern. As a response to the challenge of the world oil crisis , a study has come out which deals with the combination of diesel/bunker fuel, water and additive which was invented to make a smooth and compatible ionization effect in blending of fuel with H2O.

This research project was about an emulsified water blend in diesel fuel, mixed with diesel oil and fuel oil (bunker "C" or BFO3 and low sulfur fuel oil or LSFO). It allows the two fuels (diesel and fuel oils) to absorb water and form long-term stable hydro-oil fuel blends. When burned in a compression ignition (CI) diesel engine or fired in a steam boiler, it will result in higher energy efficiency and lower emissions.

The objective of the project is to have energy and fuel cost savings without suffering of its quality and to reduce emissions inline with the Clean Air Act.

The product has use as a water emulsion fuel in combustion for different applications:

(1) Stationary diesel engines and dual-fired boilers used in various commercial establishments (hotels, restaurants, spas, food outlets).

(2) Transport (marine).

(3) Industry and manufacturing (food, liquors, textiles, paper).

(4) Power generation.

(5) Fuel substitute for conventional diesel and high/low sulfur bunker fuel oil.

The following are the results of several experiments and testing done in this project:

Improved combustion efficiency of fuel by enhancing complete atomization of liquid fuel droplets to facilitate chemical reaction between the

carbon and hydrogen molecules with oxygen molecules to completion as carbon dioxide and water:

$$C + O_2 = CO_2 + 14{,}093 \text{ Btu/lb}$$

$$H2 + \tfrac{1}{2} O_2 = H_2O + 61{,}095 \text{ Btu/lb}$$

- Eliminates or minimizes incomplete combustion that results in energy loss, e.g. CO formation:

$$C + \tfrac{1}{2} O_2 = CO + 4{,}347 \text{ Btu/lb}$$

- With higher combustion efficiency, the resulting water addition also provides additional mass to the exhaust gas to provide greater heat transfer to boiler tubes or greater power transfer to piston of CI engines
- Higher energy efficiency means more kg steam or kWh of electricity per Liter of pure oil consumed.
- It also results in lower pollutant emissions of sulfur (as g SO_2) and carbon (as kg CO_2) per Liter of fuel.
- Pollutant concentrations (as % by volume or ppm by volume) are also lowered with the greater flue gas mass arising from water addition.

Keywords: emulsified water, combustion efficiency, sulfur dioxide, carbon monoxide and internal combustion engines.

CMPSD-2

SUPERCAPACITORS FROM NATURAL MATERIALS

Benedict C. Laguesma, Carole M. Loable, Verna Aiza S. Posada, Tristan Calasanz and Erwin P. Enriquez*

Department of Chemistry, School of Science and Engineering
Ateneo de Manila University, Loyola Heights, Quezon City, Philippines
***E-mail: epenriquez@ateneo.edu**

Researches today address the energy-depletion problem in the world by producing supercapacitors, devices that store extremely high amount of energy and discharge that energy at rates demanded by the specific application. The energy storage in supercapacitors is by static charge unlike in the electrochemical process that is used in the battery. This gives the supercapacitor advantageous properties, such as long cycle life, allowing it to be reused up to millions of times, and low impedance along with simple and rapid charging.

Here, pyrolitic carbons from seaweed polysaccharides (carrageenans, alginate, agar), banana fibers, and coconut fibers were synthesized and later used as electrode materials for supercapacitors. Chemical activation of the fibers using 10% $ZnCl_2$ or 10% KOH solutions was done to increase the surface area of the

carbonized materials, whereas no further chemical activation was done on the polysaccharides. Characterization of the samples included infrared spectroscopy, scanning electron microscopy, and BET surface area measurements.

Yields of the carbon materials were up to 72.4% for the polysaccharides, 27.6 % for banana and 55.6 % for coconut. Infrared spectra of the materials reveal functional chemical groups that are known to contribute to pseudocapacitance. The surface area obtained for carbon activated by KOH (banana, 40 m^2/g; coconut, 124 m^2/g) was higher than that for $ZnCl_2$ (banana, 18 m^2/g; coconut, 68 m^2/g) for both types of fibers, which in turn are much higher than the control or untreated fibers (banana, 8 m^2/g; coconut, 3 m^2/g). The surface area of the carbons from polysaccharides (416 to 551 m^2/g) are higher than from the banana and coconut fibers.

In turn, supercapacitor electrodes from the carbonized materials were fabricated, and these were tested by cyclic voltammetry (CV), and galvanostatic and constant power cycling (GC/CPC) using a home-built apparatus. The CV results indicate supercapacitive properties yielding a range of specific capacitances from 1.32 to 69.6 F/g for the fibers and 1.1 to 21.3 F/g for the polysaccharides. The GC/CPC for a sandwich-type electrode yielded a range of specific capacitances of 0.73 to 1.96 F/g for the fibers and 0.55 to 2.56 F/g for the polysaccharides at the current load of 1 mA and power level of 1.0 mW. These correspond to energy and power densities ranging from 0.02 to 0.73 Wh/kg and 0.15 to 0.70 kW/kg, respectively.

Keywords: supercapacitor, banana fiber, coconut fiber, carrageenan

CMPSD-3

DEVELOPMENT OF THIRD GENERATION SOLAR

John Paul B. Garcia, Katrina D. Malabanan, Jenna Riz D. Pasco and Erwin P. Enriquez*

Department of Chemistry, School of Science and Engineering
Ateneo de Manila University, Loyola Heights, Quezon City, Philippines
E-mail address of corresponding author: epenriquez@ateneo.edu

Rising costs of fuel from petroleum have increased the demand for solar cells, although the commonly available silicon-based ones remain to be prohibitively expensive for consumers. Dye-sensitized solar cells (DSSCs) are third-generation photovoltaic devices that use photosensitization of wide band gap titanium oxide nanoparticles; they offer a promising alternative to the conventional solar cell due to its great potential for low cost production making them competitive on a low cost-to-efficiency ratio. The key concerns of DSSC research include the

improvement of device performance and stability, and energy conversion efficiencies.

Here, studies on DSSC based on nanoparticles of TiO_2 (anatase) were done with the following objectives: (1) to increase the absorption band of the dye sensitizer by addition of metal ions onto crude anthocyanin extracts from *duhat* and red cabbage, (2) to diminish evaporation of the redox couple by addition of a carrageenan matrix to form a gel electrolyte, and (3) to prevent leakage of the liquid electrolyte by encapsulating the device using a silicone-based sealant.

Additions of Sn^{2+}, Cr^{3+} and Fe^{3+} showed increased absorption bands in comparison to those of the crude anthocyanin extracts. The addition of Cr^{3+} to the *duhat* dye increased the performance of the crude *duhat* dye as a sensitizer. It has also been found out that the crude *duhat* dye performed better than the *duhat* dye with Fe^{3+} ions.

Gel electrolytes consisting of a liquid iodide solution in a carrageenan matrix were prepared and incorporated into DSSC prototypes. Addition of carrageenan significantly increased the conductivity of the electrolyte system. There was no apparent improvement of device performance in terms of photovoltage, although the polymer matrix diminished the evaporation of the I^-/I_3^- redox couple, thereby improving device stability over time.

A commercial silicone sealant was used to encapsulate all sides a prototype DSSC device, ensuring that no leaks are present and the conductive sides of the device are not covered. The compatibility of the silicone sealant to the type of electrolyte solution was determined pointing to a KI/ethylene glycol electrolyte solution as most suitable. DSSC's made from 1 cm^2 electrodes generate about 0.350 mV under a halogen-lamp at 633 W/m^2 illumination. Prototype 1-cm^2 DSSC cells connected in series that produce a 1.2 V output was demonstrated to run a low-power digital device such as a digital clock.

Keywords: dye-sensitized solar cell, third generation solar cell, anthocyanins, carrageenan gel electrolyte

CMPSD-4

PHYSICOCHEMICAL AND FUNCTIONAL CHARACTERISTICS OF COCOSIN AND ITS UNIQUE EMULSIFYING BEHAVIOR

Mark Rickard N. Angelia[1], Roberta N. Garcia[2], Krisna Prak[3], Shigeru Utsumi[3] and Evelyn Mae Tecson-Mendoza[2]*

[1]Institute of Chemistry, College of Arts and Sciences
[2]Institute of Plant Breeding, Crop Science Cluster, College of Agriculture
University of the Philippines Los Baños, College, Laguna 4031
Tel.: (049) 576 0025; Fax: (049) 536 3438; Email: emtmphil@yahoo.com
[3]Laboratory of Food Quality Design and Development
Graduate School of Agriculture Kyoto University, Uji, Kyoto, Japan

The coconut is mainly cultivated as an oilseed source. It is widely distributed and abundant all year round in the Philippines. Aside from supplying oil, the endosperm is also rich in proteins. However, the coconut proteins are not utilized extensively as a source of proteins for animal and human consumption. The major coconut protein in the endosperm is the 11S globulin or cocosin.

Cocosin was purified by a combination of salt extraction, selective precipitation and gel filtration chromatography. The total globulins were composed of 73% 11S and 27% 7S. Cocosin was more soluble at different pH at high ionic strength than at low ionic strength. The 24 and 21 kD basic polypeptides of cocosin were more resistant to digestion with chymotrypsin than the 35 and 32 kD acidic polypeptide. Cocosin emulsions were most stable at 0 M NaCl, followed by emulsions in 0.1 and 0.4 M NaCl. The available SH groups of cocosin were found to be 21.6 mole SH/mole cocosin. The thermal denaturation midpoint temperature, T*m*, of the trimeric cocosin was 77.6 °C while that of the hexameric form was 100.5 °C. The percentage secondary structures of cocosin are 15.0% regular helix, 12.9% distorted helix, 10.3% regular β-strand, 11.0% distorted β-strand, 23.0% turns, and 29.0% unordered structures.

The physicochemical properties of cocosin were found to be comparable with the other 11S globulins like the soybean and pea globulins. Hence, cocosin may be used as a potential ingredient for processed foods. Moreover, the ability of cocosin to produce stable emulsions in the absence of salt is unique and could be the basis for developing new processed foods.

Keywords: coconut, 11S globulin, cocosin, physicochemical and functional properties, emulsifying behavior

CMPSD-5

PROTEIN ENGINEERING OF SULFHYDRYL GROUPS IN MUNGBEAN (*Vigna radiata* (L.) R. Wilczek) VICILIN AND EFFECTS ON ITS NUTRITIONAL AND FUNCTIONAL PROPERTIES

Mary Ann O. Torio[1*], Takafumi Itoh[2], Shigeru Utsumi[2], Roberta N. Garcia[3] and Evelyn Mae Tecson-Mendoza[3]

[1]Institute of Chemistry, College of Arts and Sciences, University of the Philippines Los Baños, College, Laguna, Philippines 4031
[2]Laboratory of Food Quality Design and Development, Graduate School of Agriculture, Kyoto University, Uji, Kyoto 611-0011, Japan
[3]Institute of Plant Breeding, Crop Science Cluster, College of Agriculture, University of the Philippines Los Baños, College, Laguna, Philippines 4031
*Corresponding author (email:meann_nilo@yahoo.com)
Tel No.: (63-49)536-2220; Fax No.: (63-49) 536-2241

Mungbean (Vigna radiata (L.) R. Wilczek) is an important grain legume. The 8S globulin or vicilin, the major storage protein in mungbean, lacks cysteine residues and disulfide bonds. Of the three isoforms of mungbean vicilin, 8Sα was found to be the major isoform, was successfully cloned, crystallized forming a rhombohedral structure and its three dimensional structure established. In this research, the 8S? globulin was engineered to introduce sulfhydryl groups and disulfide bond to improve its nutritional, structural stability and functional properties toward expanding the utilization of mungbean in processed foods. Using site-directed mutagenesis, mutants F59C, I99C and A213C were designed and prepared with free sulfhydryl group, I99C/A213C with disulfide bond and F59C/I99C/A213C with both a free sulfhydryl group and a disulfide bond, based on the established structure of mungbean 8Sα globulin. Mutants I99C/A213C and F59C/I99C/A213C formed a disulfide bond as expected which was confirmed by the Ellman method. Mutants with introduced disulfide bond exhibited greater stability to thermal denaturation and greater resistance to enzymatic digestion compared to the wild type (WT). All mutants showed greater hardness of heat-induced gels than WT, especially I99C/A213C and F59C/I99C/A213C mutants at 2% protein concentration. The results indicate that increasing sulfhydryl groups and disulfide bonds increases structural stability and functional property and thus, the modified vicilin could have new, different and wide variety of food applications.

Keywords: Protein engineering; site-directed mutagenesis; structural stability; functional property; 8S? globulin; mungbean; physicochemical properties; vicilin; *Vigna radiata*

CMPSD-6

CLASSIFICATION OF VIRGIN COCONUT OIL USING ATR-FTIR IN CONJUNCTION WITH AGGLOMERATIVE HIERARCHICAL CLUSTERING AND PRINCIPAL COMPONENT ANALYSIS

Jay O Martizano[1]*, Eugene J. Aloba[1], Vivian A. Azucena-Topor[1], April Anne H. Kwong[2] and Jhoanne Marsh C. Gatpatan[2]

[1]Department of Chemistry, College of Arts and Sciences
[2]Division of Physical Sciences and Mathematics,
College of Arts and Sciences
University of the Philippines Visayas, Miag-ao, 5023 Iloilo
TeleFax: 033-513-7020; E-mail: jay.martizano@gmail.com

Virgin coconut oil (VCO) has a potential to be one of the Philippines' high-value export products. The Philippine National Standard provided a criterion (PNS/BAFPS 22:2004) to ensure the quality of virgin coconut oil in the country.

However, the recommended methods cannot distinguish between VCO and ordinary refined, bleached and deodorized coconut oil (CCO).

This study investigated the possibility of using FTIR with an attenuated total reflectance (ATR) accessory in conjuction with chemometrics as means of distinguishing unsaturated oils, VCO and CCO. Results showed that unsaturated oils can be easily distinguished from saturated oils by observing the IR regions that indicate unsaturation at 3095-3010 cm^{-1} and 1660-1600 cm^{-1}. For olive (VOO), corn (CO), palm (PO), canola (CLO) and soybean (SO) oil sharp peaks are seen in both of these areas but no such peaks can be seen in the IR spectra of either CCO or VCO. Visual inspection, however, could not be used to distinguish VCO and CCO because their IR spectra are identical to the naked eye.

In order to take full advantage of the spectral information, including subtle features that may not be readily discerned, pattern recognition techniques such as Agglomerative Hierarchical Clustering (AHC) and Principal Component Analysis (PCA) are commonly used. These chemometrical techniques reveals relationships that were not previously suspected but can lead to interpretations that are not readily apparent by mere visual inspection of IR spectrum alone. AHC and PCA utilize subtle differences in the spectra to classify vegetable oils into different groups.

This study have shown that ATR-FTIR together with chemometrical techniques such as PCA or AHC can be used to differentiate unsaturated oils from saturated oils, and discriminate virgin coconut oil from ordinary refined, bleached and deodorized coconut oil.

List of Acronyms:

AHC - agglomerative hierarchical clustering; ATR - attenuated total reflectance; CCO - ordinary refined, bleached and deodorized coconut oil; CLO - canola oil; CO - corn oil; FTIR - Fourier Transform Infrared; PCA - principal component analysis; PO - palm oil; SO- soybean oil; VCO - virgin coconut oil; VOO - olive oil

Keywords: virgin coconut oil, FTIR, chemometrics, agglomerative hierarchical clustering, principal component analysis

CMPSD-7

OPTIMAL PROPERTIES OF LAURIC ACID IN AQUEOUS SOLUTION: A MOLECULAR DYNAMICS STUDY

Deniz P. Wong and Erwin P. Enriquez*

Department of Chemistry, School of Science and Engineering
Ateneo de Manila University, Loyola Heights, Quezon City, Philippines
E-mail address of corresponding author: epenriquez@ateneo.edu

A promising discovery about coconut oil is its antimicrobial activity, which is believed to be due to its high laureate (C-12) content. There have been

several hypotheses regarding this antimicrobial action though it is still not clearwhy the C-12, among other fatty acids of other chain lengths, yields an optimal antimicrobial property. One explanation is that the inhibitory fatty acid must be sufficiently water soluble to reach an effective concentration in the aqueous solution and yet hydrophobic enough to interact with the hydrophobic proteins or lipids on the microbial cell surface.

Here, a molecular dynamics (MD) investigation of a homologous series of fatty acids from C-8 to C-16 was done to observe any structural features that may be unique for C-12 in aqueous solution. MD simulations were done for a single fatty acid molecule (in carboxylate form) in a water box (TIP3P water model) with periodic boundary conditions using NAMD 2.6 software. VegaZZ 2.1.0 was used to prepare the molecules prior to MD calculation, and analysis of the data was done using VMD 1.8.6. We hypothesize that the length of C-12 is indeed an optimal length that minimizes the effects of competing forces that affect the stability of the fatty acid in aqueous solution., and that this may be demonstrated in mapping the hydration layers surrounding the fatty acid molecule through the radial distribution function, $g(r)$. The $g_{C_\alpha O_{H_2O}}(r)$ gives the average pair-wise separation of the C_α atom from the oxygen atoms of water (O_{H2O}) in the simulation box. The stable folded length of the fatty acid is also calculated through the.

The MD simulations reveal that all the fatty acid molecules were stable in generally stretched conformations in aqueous solution during each 1 ns simulation run. The results show high structuring of water at or near the polar carboxylate end group, as expected due to H-bonding interactions. There is also ordering of water near the methyl terminus and an apparent water depletion around the alkyl backbone, which are attributed to the hydrophobic effect.

Keywords: lauric acid, molecular dynamics simulations, radial distribution function

CMPSD-8

EFFICACY OF THE EXTRACTS OF TUBLI (*Derris elliptica*), SILI (*Capsicum* sp.), AND MALUNGGAY (*Moringa oleifera* Linn) AS PESTICIDE AND GROWTH ENHANCER OF PECHAY (*Brassica rapa* ssp. *pekinensis*)

Alexander O. Mosqueda[1*], Olive S. Anies[2], Kezia Verlyn L. Villar[3], Marites C. Bado[3] and Vidal Antonio B.Casinillo[3]

[1]Department of Chemical Engineering Technology,
[2]Department of Biological Sciences,
MSU-Iligan Institute of Technology, 9200 Iligan City, Philippines
[3]Iligan City East High School, 9200 Iligan City, Philippines
*Email: set-aom@sulat.msuiit.edu.ph

Vegetable farmers continue to use synthetic pesticides and fertilizers that contribute to pesticidal residue in the surrounding. The use of botanical materials is the most environmentally friendly practice in agricultural treatments.

Extracts from tubli roots, sili fruit and malunggay roots, in solution, were used as pesticide and growth enhancer of pechay. The botanical samples were extracted by maceration and mixed in water. Pechay plants were grown for 45 days on properly cultivated plots in a home garden, and treated with the prepared solutions at different concentrations (100% and 50%) and malathaion as standard. Treatments were applied at 10 days interval.

The efficacy of the said treatments was evaluated by comparing the areas of the pechay leaf blades and the damaged portion immediately after harvest. The leaves were flattened and overlapped with chicken wire. The areas were measured by the squares (3x3 mm) of the chicken wire taken as units. The rounded and irregular holes observed on the leaf blade were the only pest damage considered.

Results show that the treated pechay has larger leaf areas and lesser damaged portion compared to the control and standard, indicating that the extracts used can be a growth enhancer and substitute for the common commercial synthetic pesticides.

Keywords: pesticide; growth enhancer; leaf blade area; pest damage

CMPSD-9

DEVELOPMENT OF SQUID *Thysanoteuthis rhombus* INK

Cecilio S. Baga, Corazon Plete-Macachor and Rodolfo B. Burgos

Cebu State College of Science and Technology (CSCST), Main Campus
R. Palma St., Cebu City
Tel. :(032)4121141; E-mail: csbaga@yahoo.com

A squid *Thysanoteuthis rhombus* ink developed in this study is solvent-based; intermix of water, acid, glycerin, thinner and varnish used for a writing and drawing instrument. This is a liquid containing black pigment used for coloring a surface to render an image or text, drawing or writing with a pen. Experimental method of research was conducted to develop ink product with 25% squid pigment and 50% acid concentration. Based on the sensory evaluation using descriptive test by the Bachelor of Science in Industrial Technology (BSIT) major in Drafting students of Cebu State College of Science and Technology, Main Campus-College of Industrial Technology and Engineering (CITE), the Squid Ink has a moderately black color, slightly desirable solvent-like odor, ink dryness with a sharp irregular line, thick and dry ink consistency that is comparable with the commercial ink (control sample), as to color, dryness and consistency. Sensory Analysis on acceptability using the 9-point Hedonic Scale revealed that the squid inkhad like moderately rating for for color, dryness and consistency and like slightly for odor.

The color and dryness properties of squid ink had the same preference ratings with the commercial ink based on Analysis of Variance (ANOVA) and Duncan Multiple Range Tests (DMRT) at 5% level of significance. The newly developed squid ink had a density of 1.045 g/ml. The Squid Ink is generally safe for use, as revealed by the Metal Detection test result from the Department of Science and Technology (DOST) Testing Center, Region VII. The lead content detected is less than 3.10 parts per million (ppm).

Keywords: squid *Thysanoteuthis rhombus*, ink, acid.

CMPSD-10

ISOLATION OF BIOSURFACTANT FROM *SACCHAROMYCES CEREVISIAE* 2031 AND OPTIMIZATION OF FERMENTATION CONDITIONS

Ma. Leah D. Rubio[1], Nelson Villarante[1] and Virgie A. Alcantara[2]*

[1]The Department of Physical Sciences and Mathematics
University of the Philippines Manila
[2]National Institute of Molecular Biology and Biotechnology
University of the Philippines Los Baños, College, Laguna 4031
Telefax No. (049)536-2724

Biosurfactants are surface-active agents derived from microorganisms. These amphipathic molecules can either or both lower surface tension and stabilize oil in water emulsion. Biosurfactant production by different yeast isolates was investigated using glucose and waste cooking oil as substrates. Extracellular biosurfactants were not detected as evidenced by negligible emulsification activity of the culture broth after 4 days of incubation. However, heat treatment of the cells released the biosurfactant and was able to emulsify oil-in-water. From the five isolates tested, *Saccharomyces cerevisiae 2031* showed the highest emulsification activity of 58%. Optimization and partial purification of the biosurfactant gave an emulsification activity of about 76% towards kerosene. Biochemical analysis of the isolated material revealed that it is a protein-polysaccharide complex, a mannoprotein. Emulsification activity was found to vary with biomass and the amount of glucose in the culture medium.

Biosurfactants are advantageous compared to chemical surfactants due to their biodegradability, low toxicity, effectivity at extreme conditions and better environmental compatibility. Potential applications applications of biosurfactants are for bioremediationof oil and petroleum-based contaminated wastes.

Keywords: biosurfactants, *Saccharomyces cerevisiae 2031*, mannoprotein

CMPSD-11

2-PHENYLBENZIMIDAZOLE FROM THERMAL REACTIONS OF *N*-ALKYLATED *N*-PHENYL-*o*-PHENYLENEDIAMINE

Evelyn C. Creencia*[1] and Takaaki Horaguchi*[2]

[1]Department of Chemistry
College of Science and Mathematics
MSU-Iligan Institute of Technology
Iligan City 9200, Philippines
E-mail: bingsachem@yahoo.com
[2] Department of Chemistry
Faculty of Science, Niigata University
Ikarashi, Niigata 950-2181, Japan
E-mail: hora@chem.sc.niigata-u.ac.jp

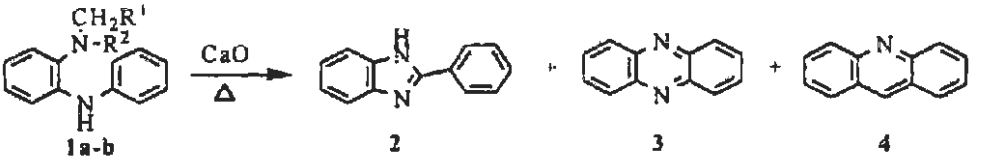

The many applications of benzimidazole and its derivatives in the fields of medicine and material science has led to numerous studies on improving the method for its synthesis. None, however, discussed thermal cyclization as an option for the synthesis of benzimidazole.

Thermal cyclization reactions of *N*-alkylated *N*-phenyl-*o*-phenylenediamine were investigated by passing vapors of the aromatic amines over calcium oxide at 450°C 560°C. The results showed that aside from the normally expected six-membered ring products of acridine **4** and phenazine **3**, the reaction also produced the unexpected 2-phenylbenzimidazole **2**.

Thermal reactions of *N,N*-dimethyl-*N'*-phenyl-*o*-phenylenediamine **1a** gave fair yields of 2-phenylbenzimidazole **2** at 450°C and 500°C (31% and 32%, respectively) which decreased radically at 560°C (14%). This is due to the fact that although imidazoles are thermally stable, they decompose at temperatures higher than 500°C. The formation of 2-phenylbenzimidazole **2** is rather unusual and may be due to an imine intermediate followed by rearrangement after cyclization. The results for *N,N*-dibenzyl-*N'*-phenyl-*o*-phenylenediamine **1b** showed good yield for phenazine **3** at 450°C (52%) and fair yields for 2-phenylbenzimidazole **2** at 450°C and 500°C (33% and 37%, respectively). Decomposition at higher temperatures become predominant, thus lowering the yields of the products.

Keywords: benzimidazole, thermal cyclization, *N,N*-dimethyl-*N'*-phenyl-*o*-phenylenediamine, *N,N*-dibenzyl-*N'*-phenyl-*o*-phenylenediamine

CMPSD-12

CHARACTERIZATION OF "SHABU" (METHAMPHETAMINE) SOLD IN ILOILO CITY

Gretchen Bo-peep G. Giner[1] and Hilario S. Taberna Jr.[2*]

[1]Philippine Drug Enforcement Agency (PDEA)
PDEA Bldg., NIA Northside Road, National Government Center
Barangay Pinyahan, Quezon City
[2]Division of Physical Sciences and Mathematics
College of Arts and Sciences
University of the Philippines Visayas
5023 Miag-ao, Iloilo
Telefax: (033) 5137020; *Email: hstaberna@upv.edu.ph

Analytical profiles (Marquis color testing, melting point, infrared spectroscopy, and gas chromatography mass spectrometry) for a transparent crystalline substance, suspected to be shabu, are established to ascertain the impurities and precursors of illegally prepared drug being sold in Iloilo City. Marquis test shows that the street sample is positive for methamphetamine. Methamphetamine was isolated and purified by acid-base extraction. Impurities were extracted with chloroform and the sample was analyzed to contain 5.06 ± 0.006 % methamphetamine. Melting point, fourier transform infrared spectroscopy (FT-IR) and gas chromatography mass spectroscopy (GC-MS) data confirm the presence of methamphetamine in the street sample and revealed ephedrine as the major adulterant.

Keywords: shabu, methamphetamine, ephedrine, Marquis test, fourier transform infrared spectroscopy, gas "chromatography" mass spectroscopy

CMPSD-13

A MATHEMATICAL MODEL OF THE CEPHALOSTATIN 1-INDUCED APOPTOSIS IN LEUKEMIC CELLS

Eva M. Rodriguez[1,3*], Ricardo C.H. del Rosario[1,2], Anita Rudy[3], Angelika Vollmar[3] and Eduardo R. Mendoza[1,4]

[1]Institute of Mathematics, University of the Philippines, Diliman, Quezon City
[2]Department of Membrane Biochemistry
Max-Planck Institute of Biochemistry, Martinsried, Germany

E-mail address: rcdelros@gmail.com.
[3]Department of Pharmacy and Center for Drug Research
Ludwig-Maximilians University, Munich, Germany
E-mail: anita.rudy@cup.uni-muenchen.de, angelika.vollmar@cup.uni-muenchen.de.
[4]Physics Department and Center for NanoScience
Ludwig-Maximilians University, Munich, Germany
E-mail: mendoza@lmu.de.
[5*]Department of Mathematics, University of Asia and the Pacific
Pearl Drive, Ortigas Center, Pasig City 1605
Tel.: 637-0912 loc 277 or 278; Fax: 637-0912 loc 369; E-mail: emrod3@yahoo.com.

Understanding the mechanisms involved in apoptosis has been an area of extensive study due to its critical role in maintaining a homeostatic balance in multicellular organisms as a response to pro- or anti-apoptotic stimuli. Our special interest lies in understanding the apoptosis of tumor cells which are mediated by novel potential drugs. Cephalostatin 1 is a marine compound that induces apoptosis in leukemic cells in a dose- and time-dependent manner at nanomolar concentrations using a novel pathway that excludes the receptor-mediated pathway and includes both the mitochondrial- and ER-mediated pathways. In this study, the methods and tools of Petri net theory were used to construct, analyze, and validate a discrete Petri net model for cephalostatin 1-induced apoptosis.

Based on actual experimental results from the Vollmar laboratory and literature search, we constructed a discrete Petri net model consisting of 43 places and 59 transitions using a software tool called Snoopy. Standard Petri net analysis techniques such as structural and invariant analyses and modularity analysis via abstract dependent transition sets (ADT-sets) were employed using the software tool called Charlie. Results of these analyses demonstrated model consistency with known biological behavior. The sub-modules represented by the maximal ADT-sets are comparable with the functional modules of apoptosis identified by Alberghina and Colangelo. Moreover, by its readability, the Petri net model revealed a primary role for the ER-mediated pathway in cephalostatin 1-induced apoptosis, which can be verified by further experimentation.

Keywords: apoptosis, cephalostatin 1, discrete Petri net, invariant analysis, maximal ADT-sets, modularity analysis, structural analysis

CMPSD-14

IN VITRO GLUTATHIONE CONJUGATION OF SULFANILAMIDE ANTIBIOTICS WITH GLUTATHIONE TRANSFERASE

Elmer-Rico E. Mojica[1*] and Diana S. Aga[2]

[1]Institute of Chemistry, College of Arts and Sciences
University of the Philippines Los Baños, College, Laguna 4031
[2]Department of Chemistry, University at Buffalo
State University of New York, Buffalo, NY, USA 14260
*Email address: elmericomojica@yahoo.com, dianaaga@buffalo.edu

Glutathione (GSH) is a tripeptide present in biological systems. It plays an important role in the detoxification of electrophilic foreign compounds and chemically reactive intermediates, which may arise during the biotransformation of xenobiotics. Conjugation reactions with GSH have been suggested as an important pathway of contaminant transformation, particularly in the pesticide literature. Glutathione conjugation or reaction with chemicals is catalyzed by glutathione S-transferase (GST) enzymes. GST enzymes are dimeric, mainly cytosolic, enzymes that have extensive ligand binding properties in addition to their catalytic role in detoxification and are present in most organisms including plants, animals, protozoa, fungi and bacteria. In this study, GSH was reacted with different sulfanilamide antibiotics *in vitro* with GST from equine liver. Sulfonamides used includes sulfamethizole (SMZ), sulfamethoxazole (SMX), sulfamethazine (SAZ), sulfadimethoxine (SDM), sulfathiazole (SFT), sulfadiazine (SFD) and sulfisoxazole (SFX). Results of liquid chromatography-mass-spectrometry (LC-MS) showed formation of glutathione adduct (GSH-sulfonamide product) in all samples with a pattern of GSH + sulfonamide + 13. LC-MS/MS of the samples showed GSH as one of the fragment that is formed. Neutral loss of water, glycine and glutamic acid was also observed in almost all samples. The same results were also obtained when partially purified GSTs from plants were used.

Keywords: glutathione, mass spectrometry, sulfanilamide

CMPSD-15

MOLECULARLY IMPRINTED POLYMER MICROSPHERES FOR THE SELECTIVE EXTRACTION OF ARTEMISININ

Christian A. Malapit*, Kendricks S. Lao and Regina C. So

Department of Chemistry, Ateneo de Manila University,
School of Science and Engineering, Loyola heights, Quezon City 1108
Email: cmalapit@ateneo.edu

Malaria causes about two million deaths a year worldwide according to World Health Organization. Artemisinin, a sesquiterpene, endo-peroxide lactone was found as one of the most potent anti-malarial drug at hand nowadays. An efficient method for extracting artemisinin is a serious concern to supply the need of 500 million malaria cases occurring annually worldwide. One such method to address this problem is by molecular imprinting technique.

Molecular imprinting is an efficient technique to introduce specific molecular recognition sites into a polymer matrix which can be applied for chromatographic separation and chemical sensing.

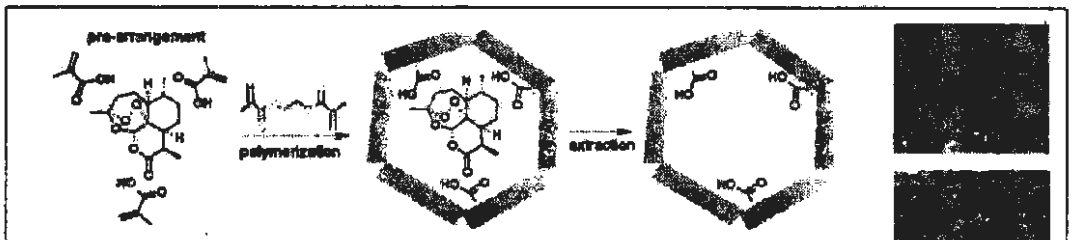

Fig. Molecular imprinting process for artemisinin

In this study, molecularly imprinted polymers (MIPs) were synthesized by traditional bulk polymerization and solid polymer blocks were obtained. Grinding and sieving of these polymers resulted to particles with irregular size and shape and low yield. New polymerization strategies have been proposed and one of the simplest formats is by precipitation polymerization.

Precipitation polymerization was investigated and uniformly-sized, micro-spherical artemisinin-imprinted polymers were obtained from acetonitrile (95%vol). The method was further developed to tune-in the morphology of the polymers. SEM and BET analysis showed that the size and porosity of polymers can be controlled by dilution and addition of toluene as co-solvent. Heat and UV polymerization was used, the type of monomer, and template/monomer ratio were optimized. The polymer prepared by 5:6:20 artemisinin/methacrylic acid/ethylene glycol dimethacrylate ratio in 5%toluene/acetonitrile (95%vol) solvent binds artemisinin with the highest selectivity. An equilibrium and non-equilibrium and

non-equilibrium binding isotherm study of the polymer was also established. Furthermore, these polymers were applied in solid-phase extraction of artemisinin from *Artemisia annua* plant extract.

Keywords: molecular imprinting, precipitation polymerization, artemisinin (quinghaosu)

CMPSD-16

A MATHEMATICAL MODEL OF RESPIRATION IN *HALOBACTERIUM SALINARUM*

Cherryl O. Talaue[1], Ricardo C.H. del Rosario[1,2,*], Eduardo Mendoza[3,4] and Dieter Oesterhelt[2]

[1]Institute of Mathematics
University of the Philippines Diliman, Quezon City, 1101, Philippines
Tel./Fax : +632-920-1009
E-mail: cherryl@math.upd.edu.ph, che1002@yahoo.com, rcdelros@math.upd.ph
[2]Max Planck Institute of Biochemistry,
Department of Membrane Biochemistry
Am Klopferspitz 18, 82152 Martinsried, Germany
Tel.: +49-89-8578-2368, Fax: 49-89-8578-3557
E-mail: rcdelros@biochem.mpg.de, oesterhe@biochem.mpg.de
[3]Department of Computer Science
University of the Philippines, Diliman, Quezon City 1101, Philippines
[4]Physics Department & Center for Nano-Science
Ludwig Maximilians University
Gewchister-Scholl-Platl 1, 80539 Munich, Germany
E-mail: Mendoza@lmu.de

Halobacterium salinarum is a rod-shaped halophilic archaeon which can live under four bioenergetic regimes, namely, aerobic respiration, photosynthesis, anaerobic respiration and arginine fermentation. It is considered a model organism for photosynthesis due to its simple mechanism for energizing the membrane: it has a light-driven retinal-containing proton pump bacteriorhodopsin which is the simplest known proton pump in nature. The protons pumped via the electron transport chain also enhance the electro-chemical potential which the ATP synthase utilizes to drive ATP synthesis. In this work, we present a mathematical model of respiration in *H. salinarum* using the mathematical modeling framework of Generalized Mass Action (GMA) which one of the variants of Biochemical

Systems Theory (BST). Due to lack of kinetic data for aerobic respiration in *H. salinarum* we used the GMA modeling framework since knowledge of the exact mechanisms of each reaction is not required to set up the equations. Models can be designed based on the identity of the reactants and their reactional and regulatory interconnections.

Light inhibition of respiration in H. salinarum has been studied in the 70s and our model will later be used to understand the interaction of these two bioenergetic processes. Our current results can exhibit the few published data on respiration (i.e., oxygen consumption and phosphorylation) on this organism. Aside from the reactions and pumping of the complexes in respiration, our model also includes the sodium-proton antiport, the potassium uniport and the dynamic changes of the membrane potential and ΔpH. The exact nature of the sodium-proton antiport in H. salinarum is still not well understood hence we will consider two types, an electro-neutral antiporter and an electrogenic one and we present the model output for each one.

Keywords: Bioenergetics, respiration, oxidative phosphorylation, Halobacterium salinarum, Biochemical Systems Theory

CMPSD-17

THERMAL STABILITY AND CHARACTERIZATION OF A PARTIALLY PURIFIED LIPASE FROM *GEOBACILLUS SP.* M5

Ma. Cristina M. Baisauli[1], Virgie A. Alcantara[2], Marcelina Lirazan[1] and Jessica F. Simbahan[2*]

[1]Department of Physical Sciences and Mathematics, UP Manila
[2]National Institute of Molecular Biology and Biotechnology
University of the Philippines Los Baños, College, Laguna 4031
Telefax: (049)536-2724

Lipids are biological compounds that are non-polar and are poorly soluble or insoluble in water. They constitute a large part of the earth's biomass and of waste products from industrial processes. Lipolytic enzymes, or lipases, play an important role in the degradation of these water-insoluble compounds. *Geobacillus sp.*, M5, a microorganism isolated from a hot spring in Albay, has been identified to produce high amounts of an extracellular lipase. However, little has been done to purify the enzyme. It is the objective of this study to partially purify the enzyme and determine its stability at different temperatures. The lipase was partially purified by microfiltration and ammonium sulfate precipitation. Thermal stability was determined after each purification procedure at 55°C, 30°C, 4°C and -20°C.

The crude lipase from microfiltration retained 96 % of its activity after 90 minutes of incubation at 55°C, 49% activity after 18 hours at 30°C, 46% activity after 5 weeks at 4°C and 61% activity after 5 weeks at -20°C. The ammonium sulfate precipitated lipase retained 90% activity after 60 minutes at 55°C, 99% activity after 15 hours at 30°C, 100% activity after 5 weeks at 4°C and 92% at -20°C. The stability of the crude and ammonium sulfate lipase at 55 °C indicate that it can be used in industrial processes that require high operational temperatures.

Keywords: extracellular, Lipolytic enzymes, *Geobacillus sp,* microfiltration

CMPSD-18

EFFECT OF PROTEIN STRUCTURE DISRUPTING AGENTS AND METAL IONS ON THE ACTIVITY OF PARTIALLY PURIFIED THERMOPHILIC LIPASE FROM *GEOBACILLUS* SP., M5

Ma. Therese Anne L. Domingo[1], Virgie A. Alcantara[2], Nelson Villarante[1] and Jessica F. Simbahan[2]*

[1]The Department of Physical Sciences and Mathematics, UP Manila
[2]National Institute of Molecular Biology and Biotechnology
University of the Philippines Los Baños, College, Laguna 4031
Telefax: (049)536-2724

Lipases catalyze the hydrolysis of triacylglycerols to glycerol and free fatty acids at an oil-water interface. Presence of compounds and metal ions, as well as the temperature and pH of the reaction mixture are important factors that affect the activity of the enzyme. The effect of protein structure disrupting agents and metal ions on the activity of thermophilic lipase from *Geobacillus* sp. M5 was investigated in the view of its potential application in wastewater treatment. Lipase was isolated from *Geobacillus* sp. M5 by ammonium sulfate precipitation followed by dialysis. Lipase characterization was performed on the dialyzed enzyme. The optimum temperature and pH for *Geobacillus* sp. M5 lipase was found to be at 55°C and 7.0, respectively. Lipase activity was least affected by DTT, retaining 93.103% of its activity even at 10 mM of the compound. The lipase activity inhibited by 20% upon addition of SDS and Tween80 but was most inhibited by EDTA. Activity was decreased more than half by addition of 1 mM EDTA. The effect of metal ions on the enzyme was also investigated. Lipase activity was decreased by 21.5% in the presence of sodium but was enhanced slightly in the presence of magnesium. The high activity of lipase produced by *Geobacillus* sp. M5 plus its resistance to different effectors indicated the potential of this enzyme to be used in wastewater treatment.

Keywords: *Geobacillus* sp, triacylglycerols, thermophilic

CMPSD-19

STOCHASTIC DIFFUSION OF B-LYMPHOCYTES IN A 1-DIMENSIONAL SHAPE SPACE

Christine Joy G. Gravino* and Mark Nolan P. Confesor

Physics Department, Mindanao State University -
Iligan Institute of Technology
A. Bonifacio Avenue, Tibanga, 9200 Iligan City, Philippines
*Email: ceejay@physics.msuiit.edu.ph

The body's immune system is a complex network of cells and tissues where the *B-lymphocytes* or *B-cells* play an important role. The diversity of the immune system is further increased to facilitate the detection of mutating antigens. Furthermore, due to limited resources, *B-cells* undergo somatic hypermutation to recognize evasive antigens. In 1979, Perelson and Oster introduced a simple way of modeling the antibody-antigen interaction through the shape space formulation (Theoretical Studies of Clonal Selection: Minimal Antibody Repertoire Size and Reliability of Self-Non-self Discrimination, J. Theor. Biol. (1979) 81, 645-67). And in the works of Perelson and Wiegel, they modeled the mutation of *B-cells* as diffusion in shape space (Perelson S., Wiegel, F., Some Design Principles for Immune System Recognition, Complexity, John Wiley and Sons, Inc., Vol. 4, No. 5, 1999).

In this work, we present the stochastic white noise calculation of the diffusion of *B-cells* in a one dimensional shape space. To describe the proliferation of antibody producing cells and their diffusion in shape space due to antibody gene mutation, we denote $b(S, t)$ as the density in shape space of *B-cells* with shape S at time t that have been stimulated by antigen. For a 1-dimensional case, we obtain the *B-cell* density as

$$b(S,t) = \frac{1}{\sqrt{4\pi Dt}} exp\left(-\frac{(S_B - S_A)^2}{4Dt} \right)$$

The time of detection of the antigen by the *B-cells* can be calculated using the formula obtained by Perelson and Wiegel in their studies on "Some Design Principles for Immune System Recognition". We take note that the above result resembles to the propagator of a free particle in quantum mechanics.

Keywords: B-lymphocytes, diffusion, shape space

CMPSD-20

DETECTION OF WILSON'S DISEASE BY ATOMIC ABSORPTION SPECTROPHOTOMETRIC ANALYSIS OF SERUM AND URINARY COPPER AND CERULOPLASMIN ANALYSIS

Ma. Cristina B. Portilla[1], Jason Paul C. Monlinong[1], Cherrie B. Pascual[1,2] and Abdias Aquino[3]

[1]Research and Biotechnology Division, St. Luke's Medical Center
279 E. Rodriguez Sr. Blvd, Cathedral Heights, Quezon City 1102
Tel.: 723-0101 local 4501; Telefax 726-0467
[2]Institute of Chemistry, University of the Philippines,
Diliman, Quezon City 1101
[3]Institute for Neurosciences, St. Luke's Medical Center,
Quezon City 1101

Healthy people can excrete unwanted copper in the body but those with Wilson's disease cannot. Wilson's disease is a rare autosomal recessive inherited disease that causes copper poisoning. In persons affliced with this disease the mechanism of copper transport and excretion by the liver is impaired and there is progressive build up of copper primarily in the liver or the brain.

In addition to evaluation of clinical symptoms, analyses of copper in both serum and urine are utilized for detection of Wilson's disease. 24-hour urine and serum samples from different patients were analyzed for copper using flame atomic absorption spectrophotometry (AAS) after acid digestion of samples. Samples from patients with Wilson's disease had very high 24-hour urine copper levels (exceeding 60 µg/day) and their serum free copper concentrations were below normal values of 0.7 1.4 µg/ml.

This paper will also present a case of Wilson's disease in a Filipino family of three male siblings. Two of the males have the disease while the middle one is disease-free. Both have abnormally high 24-hour urine copper levels (968 and 585 µg/day vs max. of 60 µg/day for normal values). The serum free copper concentrations (0.21 µg/ml or less) were below normal values of 0.7-1.4 µg/ml. Their 24-hour urine copper levels were also monitored with drug therapy. With drug therapy, the levels of 24-hour urinary copper decrease to values approaching normal values.

Keywords: Wilson's disease, atomic absorption spectrophotometry, copper

CMPSD-21

CHARACTERIZATION AND SOURCE IDENTIFICATION OF AMBIENT AIR PM_{10} IN VALENZUELA CITY SAMPLING SITE

Flora L. Santos*, Preciosa Corazon B. Pabroa, Joseph Michael Racho and Ryan P. Morco

Philippine Nuclear Research Institute
Department of Science and Technology
Tel.: 96011 loc. 281, (02)9267343; *E-mail: flsantos@nri.dost.gov.ph

Air pollution in Metro Manila (in particular, in Valenzuela City, a highly industrialized area) and its adverse impacts to health is a source of concern to various stakeholders. The research aims to help address the problem by providing scientific data (in particular, the major sources of particulate pollution) on which to base policies to improve air quality.

Particulate matter of most concern with regard to adverse effects on human health are generally <10 um in size and are referred to as PM_{10}. PM_{10} samples were collected on Nuclepore filters [8μm pore size for the coarse or $PM_{10-2.5}$ fraction and 0.4μm for the fine or $PM_{2.5}$ fraction] using a Gent sampler. Particulate mass is determined by gravimetry using a micro analytical balance (Mettler MT5) with 1μg sensitivity. Elemental levels in air particulate samples are determined using non-destructive nuclear (or related) multielement analytical technique using an energy-dispersive x-ray fluorescence spectrometry (EDXRF) (Kevex 771-EDXRF Spectrometer).

Data for Valenzuela City sampling site show the presence of Pb in both the coarse and the fine fractions with levels relatively higher as compared with other sampling sites such as in Ateneo, Poveda and NAMRIA sampling sites. Source apportionment (using the Positive Matrix Factorization) of the Valenzuela City data distinctly shows a Pb source factor in both the coarse and the fine fractions. Conditional probability function (CPF) of Pb values from Valenzuela City in 2005 indicates large source contributions coming from the surrounding area of the sampling station particularly about NNW-N, ENE-E and SSE-W of the sampling station. Results in Valenzuela City indicate the need to do a more comprehensive evaluation of the area to determine the sources of Pb and formulate measures to bring down ambient levels.

Keywords: metro manila, admu, namria, poveda, valenzuela city, pm10, pm2.5, source apportionment

CMPSD-22

BIOSORPTION OF CADMIUM, COPPER AND LEAD BY *Gracilariopsis bailinae* BIOMASS

Steve P. Janagap[1,2*] and Jay O. Martizano[1]

[1]Department of Chemistry, College of Arts and Sciences
[2]Institute of Aquaculture, College of Fisheries and Ocean Sciences
University of the Philippines - Visayas, 5023 Miagao, Iloilo
*E-mail: spjanagap@upv.edu.ph

Equilibrium contact experiments were conducted to determine the ability of dried *Gracilariopsis bailinae* to remove cadmium (Cd^{2+}), copper (Cu^{2+}) and lead (Pb^{2+}) in water. Analysis of the metals was carried out using atomic absorption spectroscopy. The outstanding function of the biosorbent for Cd^{2+}, Cu^{2+} and Pb^{2+} was demonstrated at pH 5 and were fitted to the Langmuir and Freundlich isotherms. The Langmuir model was only applicable to cadmium biosorption (R^2 = 0.988) with maximum uptake capacity (q_{max}) and affinity constant (b) equal to 15.02 mg g^{-1} and 0.0217 L mg^{-1}, respectively. The Freundlich model fitted the biosorption data for the three metals with R^2 ranging from 0.900 to 0.990 and the order of adsorption capacity (K) and intensity (m) of *G. bailinae* for the metals were Pb > Cd > Cu and Pb > Cu > Cd, respectively.

The Fourier-transform infrared spectra of the *G. bailinae* and the metal-loaded biomass were obtained to determine the chemical groups present, which may be involved in the biosorption of the heavy metals. It was found that amide and sulfate groups were present in the biomass which could be responsible for the biosorption. *G. bailinae* can be a potential biosorbent for heavy metals especially for lead.

Keywords: *Gracilariopsis bailinae*, biosorption, metals, Langmuir, isotherm

CMPSD-23

MONITORING PETROLEUM HYDROCARBONS IN SEDIMENTS USING TOTAL SOLVENT EXTRACTABLE MATERIALS (TSEM)

Hilario S. Taberna Jr.*, Ida G. Pahila, Jay O. Martizano and Leandro T. Gamarcha

Division of Physical Sciences and Mathematics
College of Arts and Sciences
University of the Philippines in the Visayas
5023 Miag-ao, Iloilo
Telefax: (033)5137020; *Email:hstaberna@upv.edu.ph

There are many analytical techniques available to measure total petroleum hydrocarbon (TPH) concentrations in the environment and one of the major problems that we encountered in the assessment of petroleum hydrocarbon contamination due to oil spill is the absence of common approach to determine TPH levels in sediments. The usual practice is to use the oil and grease method (US EPA Method 9017b) to establish the amount of petroleum hydrocarbons in sediments. However, we found out that the n-hexane extractable materials (HEM) were non-specific to petroleum hydrocarbons as revealed by the FTIR spectra of the HEM and the standard oil sample. Moreover, HEM values were not correlated with polycyclic aromatic hydrocarbons thus making it a poor method in assessing the severity of petroleum contamination. Accordingly, we looked for an alternative method that is the TSEM, as described by Wang and Fingas (1994) and tested for monitoring. We found out that the TSEM method has high recovery (82 87 %) in the spiked samples of wide range of concentrations, (100 µg/g 10000µg/g). TSEM values are highly correlated with PAHs within six months after the oil spill and also highly correlated with TPH values determined using FTIR. The FTIR spectra of the TSEM are similar to the standard oil sample and this result implies that material extracted is mostly petroleum hydrocarbons. The study has established that TSEM is a good method to monitor petroleum hydrocarbons in sediments.

Keywords: total petroleum hydrocarbons, hexane extractable materials, total solvent extractable materials, monitoring

CMPSD-24

APPLICATION OF THE FENTON'S PROCESS ON THE REDUCTION OF COLOR AND COD OF TEXTILE WASTEWATER CONTAINING DIRECT ORANGE 26 DYE

Jovita. L. Movillon, Jerico R. Aguila, Sixto A. Valencia and Charisse M. Mendoza

Department of Chemical Engineering
College of Engineering and Agro-industrial Technology
University of the Philippines Los Baños, College, Laguna

The textile industry is one of the leading industries in the Philippines. Its export earnings of about US $ 3 B corresponds to an average of 8% of the total export earnings. Textile processing uses a variety of chemicals, depending on the nature of the raw materials and products, which include different proteins, detergents, dyes, acids, sodas, salts and metals which are not degradable into non-toxic end products. The textile factories, like other factories, are required to treat their effluent before discharge, in compliance to DENR Administrative Order No. 35 which limits the COD and BOD level to 150 and 300 mg/L, respectively. Likewise, color and turbidity should be reduced, as these could cause aesthetic problem and real hazard to the environment. Residual dye in textile wastewater pose problem in absorption and reflection of sunlight entering the water. Hence, too much color, indirectly interferes with the growth of bacteria to levels insufficient to biologically degrade impurities in water. It may also hinder the photosynthetic activity of aquatic plants.

Chemical Treatment:

Oxidative treatment, under the chemical treatments available, usually gives better results and promising outcome because it involves the degradation process of wastewater contaminants (Ciardelli, 1998). One of these oxidative treatments is the Fenton's process. The effectivity of this treatment was studied on a simulated textile wastewater. This type of textile dye was chosen for its availability in the market. The effect of varying certain amount of factors of the process was considered. Thus, color removal and the COD reduction reflect the effects of varying these factors.

Objectives:

This study generally aimed to evaluate the application of Fenton's process on the treatment of simulated textile wastewater containing Direct Orange 26. Specifically, the study aimed to:

1) determine the pH, color and COD of the simulated wastewater;
2) determine the effect of varying the amount of H_2O_2 on the reduction of COD;

3) evaluate the effect of varying the amount of $FeSO_4 \cdot 7H_2O$ solution, which contained the catalyst, Fe^{2+}, on the reduction of COD;
4) assess the effect of varying the concentration of the simulated textile wastewater on the reduction of COD; and
5) propose a degradation mechanism of the reaction of Direct Orange 26 with Fenton reagent.

Summary and Conclusion:

The treatment of simulated textile wastewater containing Direct Orange 26 was conducted using the Fenton's process. Varying the amounts of the Fenton's reagent, such as Hydrogen peroxide and iron catalyst, was made to determine the effect on COD and color. Different amounts H_2O_2 (5, 10, 15 and 20 mL) and iron catalyst (2, 4, 6 and 8 mL), and different concentrations of simulated textile wastewater (4000, 5000, 6000 and 7000 ppm) were used. The COD level and color of the treated wastewater were measured. The highest percent COD reduction was 98.48% and was obtained from the ratio 4:15:20 (mL of iron catalyst: mL of H_2O_2: mL of wastewater), with a 5000 ppm concentration of the simulated textile wastewater. The treated wastewater was completely decolorized. The degradation mechanism was proposed with the possible end products. The Fenton's process was found to be an effective treatment for this kind of wastewater.

Keywords: Fenton, reagent, textile wastewater

CMPSD-25

APPLICATION OF ION TRAP-MASS SPECTROMETRY IN MONITORING CHANGES IN ACTIVATED SLUDGE PHYSIOLOGY UPON EXPOSURE TO TOXIC COMPOUNDS

Elmer-Rico E. Mojica[1*] and Diana S. Aga[2]

[1]Institute of Chemistry, College of Arts and Sciences
University of the Philippines Los Baños, College, Laguna 4031
[2]Department of Chemistry, University at Buffalo
State University of New York, Buffalo, NY, USA 14260
Email:elmericomojica@yahoo.com, dianaaga@buffalo.edu

The activated sludge process is the most commonly used biological wastewater treatment technology employed. Microbial communities in activated sludge usually undergo different physiological and structural modifications upon exposure to toxic chemicals. One modification might lead to the release of chemicals/metabolites as specific response to a given toxic compound, which could serve as biomarker for that particular toxicant. The purpose of this study is to apply liquid chromatography with ion trap mass spectrometry to monitor the changes on the composition of the soluble fraction of activated sludge mixed liquor after

exposing to different toxic chemicals. Toxic chemicals used include heavy metals like lead and cadmium and organic compounds such as chlorodinitrobenzene, dinitrotoluene and dinitrophenol. Results indicated the formation of several peaks not found in untreated samples. Looking at the peaks revealed the appearance of high molecular weight compounds which could be fragments of biomolecules (proteins or polysaccharides) that are usually expressed by microorganisms when exposed to toxic chemicals. These results provide insight on the potential of LC-IT-MS to monitor the rapid changes in the activated sludge physiology upon exposure to toxic compounds. It could also be used as an early warning instrument of upset events in activated sludge.

Keywords: activated sludge, mass spectrometry, organics

CMPSD-26

COMPARATIVE TREATABILITY STUDIES FOR THE DECOLORIZATION AND COD REMOVAL OF SUGAR REFINERY SPENT ION-EXCHANGE-PROCESS (SIEP) EFFLUENT

Jewel A. Capunitan[1*], Catalino Alfafara[1], Veronica Migo[2], Jovita Movillon[1], Erlinda I Dizon[3] and Masatoshi Matsumura[4]

[1]Department of Chemical Engineering
[2]National Institute of Molecular Biology and Biotechnology
[3]Institute of Food Science and Technology
University of the Philippines Los Banos, College, Laguna 4031
Telefax: (049)-536-2315; * E-mail: jwl103@yahoo.com
[4]Institute of Applied Biochemistry
University of Tsukuba, Tennodai 1-1-1, Tsukuba City 305-0006, Japan

Treatability studies were conducted for the decolorization and COD removal from Sugar-Refinery-Spent-Ion-Exchange-Process (SIEP) effluent by electrochemical oxidation electrochemical coagulation/flocculation.
Batch electrolysis experiments were conducted at different operating currents, and removal efficiencies for color and COD were evaluated. With sintered platinum as the anode, the electro-oxidation of SIEP effluent at 3 and 5 Amperes resulted to more than 99 percent decolorization efficiency after 7 hours of treatment. For both currents, the decolorization efficiency increased with the treatment time but leveled off during the 6th hour at 3 Amperes and during the 3rd hour at the 5 Amperes operating current. Higher decolorization efficiency was observed at 5 Amperes than at 3 Amperes since higher amount of oxidants was produced as the current was increased. The COD removal efficiency also increased with time, indicating that

the organic matter removed corresponds to the color removed from the SIEP effluent. In electroflocculation, the Al^{3+} flocculants generated from an aluminum anode removed as much as 75 percent of the color at 5 Amperes operating current for 8 hours electrolysis time. However, no significant differences were observed between the decolorization efficiencies and COD removal efficiencies at the 3 Amperes and 5 Amperes operating currents. An increasing trend in both the decolorization and COD removal efficiencies with time was also observed.

Based on the results, electro-oxidation proved to be more effective method in removing color and COD from the SIEP effluent than electroflocculation.

Keywords: electrooxidation, electroflocculation, spent ion-exchange-process effluent

CMPSD-27

ELECTROCHEMICAL TREATMENT OF TANNERY WASTEWATER

Jemma Rose K. Aguado[1*], Catalino G. Alfafara[1], Veronica P. Migo[2], Jewel A. Capunitan[1], Monet Concepcion C. Maguyon[1] and Masatoshi Matsumura[3]

[1]Department of Chemical Engineering
[2]National Institute of Molecular Biology and Biotechnology
University of the Philippines Los Banos, College, Laguna 4031
Telefax: (049)-536-2315; E-mail: aguado_jr@yahoo.com
[3]Institute of Applied Biochemistry
University of Tsukuba, Tennodai 1-1-1, Tsukuba City 305-0006, Japan

The feasibility of electrochemical treatment to remove total chromium and COD from tannery wastewater was investigated. Electrocoagulation was done for chromium removal while electrooxidation was used as a second-stage treatment for COD removal.

Complete chromium removal was obtained using 2A operating current after 3 hours electrocoagulation. Adsorption of chromium ions onto aluminum hydroxide flocs generated (from the dissolution of aluminum anode and it reaction with hydroxyl ions generated at the cathode) was considered the major mechanism for removal. This was because the pH of the wastewater was in the range where chromium does not precipitate as its metal hydroxide, but was favorable for the precipitation of aluminum hydroxides. Charge dose defined as the amount of electricity required to remove a unit mass of chromium by electrocoagulation was found to be inapplicable as a scale-up factor in this process. An alternative strategy to charge dose was explored for scale up/operation based on the relationship between volumetric current and kinetic rate constant (found to be first-order by the integral method).

Electrooxidation, as a second-stage treatment for COD removal, could obtain a COD removal efficiency of 34% in 3 hours at 4A operating current. However, a COD level conforming to DENR effluent standards could still be possible by extending the electrolysis time. The concept of charge dose for COD removal was found applicable and could be used as a useful factor for operation and scale-up.

Keywords: electrocoagulation, electrooxidation, electrolysis, tannery wastewater, chromium, charge dose

CMPSD-28

DIFFERENTIAL EXPRESSION OF A NOVEL BANANA MADS-BOX GENE SHOWS DEVELOPMENTAL CONTROL OF CLIMACTERIC FRUIT RIPENING

Eureka Teresa M. Ocampo[1]*, Haya Friedman[2], Edna Pesis[2] and Evelyn Mae Tecson-Mendoza[1]

[1]Institute of Plant Breeding, Crop Science Cluster, College of Agriculture
University of the Philippines Los Baños, College, Laguna, Philippines 4031
Tel: (63) 49 5760024 to 25; Fax: (63) 49 536 3438;
*E-mail: eteresaocampo@yahoo.com
[2]Department of Postharvest Science of Fresh Produce, Agricultural Research Organization,
The Volcani Center, Bet Dagan, Israel 50250

The regulatory role in ripening of a novel banana fruit-specific MADS-box[3] gene was investigated by quantification of its expression and correlation to the rise in ethylene production during fruit maturation. The gene, *MAMADS2*, was isolated from ripe banana fruit cDNA and had a putative protein sequence that was structurally similar to Type II MADS-box transcription factors that are implicated in key developmental processes.

Using real time PCR analysis, *MaMADS2* expression was quantified in banana pulp and peel tissues sampled during ripening of bananas stored in 95% (high) and 82% (low) relative humidity (RH). Ethylene and CO_2 production were measured from whole fingers and tissues using headspace gas analysis. *MaMADS2* expression was relatively high only in the pulp under both storage conditions ranging from 15% to 167% relative to expression in peel at 2 days of high RH storage. The expression in pulp tissues increased from 6 to 10 days in high humidity storage followed by a decline in levels. The corresponding ethylene climacteric peak occurred on the 9th day. In the peel, increases in ethylene were observed only on the 12th day of storage. The highest relative expression (167%) was observed at 2 days after low RH storage indicating that the gene is responsive to environmental stress. Under low RH, pulp ethylene production was lower but fruit deterioration

was earlier. This indicates an earlier developmental shift to the ripening stage brought about by the low moisture conditions.

The results conclusively show that *MAMADS2* is already expressed before the initiation of ripening with maximum expression levels corresponding to the ethylene climacteric peak. *MaMADS2* may thus act in the developmental regulation of banana ripening.

[3]MADS-box- MADS is derived from the initials of the founder proteins Minichromosomal maintenance1, Agamous, Deficiens and Serum Response Factor

Keywords: MADS-box, developmental factors, banana, ripening, climacteric

CMPSD-29

ADSORPTION CAPACITY OF CARBONIZED RICE HUSK BAMBOO CHARCOAL OF NITRATE NITROGEN

Rosana E. Espiritu[1*] and Hitoshi Kosuge[2]

[1]Philippine Rice Research Institute
Maligaya, Science City of Muñoz, Nueva Ecija,
Tel.: (044) 456-0433 loc 311, E-mail: reespiritu@philrice.gov.ph
[2]Department of Chemical Engineering
Tokyo Institute of Technology, Tokyo, Japan,

The contamination of the groundwater with nitrate is becoming a global issue that can be pinned down from man-made sources such as intensive use of nitrogenous fertilizers, septic tank effluent, industrial wastewater, and leachate from landfills resulting in the formation of methemoglobin, and nitrosamine.

Several technologies have already been developed for nitrate removal from drinking water, however, their applications are in large scales. Thus, the focus of this study is to explore the potential of adsorption using carbon from bamboo and rice husk owing to lower production cost and assured availability of materials.

Consequently, adsorption isotherms of NO_3-N using bamboo charcoal (BC) and carbonized rice husk (CRH) from aqueous medium have been investigated. BC and CRH were prepared by HCl-treatment (BC1) and CO_2 activation (BC2), and HCl- (CRH1) and NaOH&HCl (CRH2)- treatment, respectively. Results showed that NO_3-N adsorption of BC and CRH exhibited maximum adsorption values at pH 3.0. Moreover, adsorption performance of BC1 and CRH1 was mainly influenced by the electrostatic interaction between the positively-charged surface of both adsorbents, and negative charge of nitrate ions. On the other hand, adsorption performance of BC2 was mainly influenced by the large surface area of 1029 m^2/g, while CRH2 was due to the increased fixed carbon as influenced by the leaching

process with NaOH. The adsorption equilibrium studies for all the adsorbents were examined at pH 3.0 under constant temperature of 30°C, and isotherms were determined and correlated with Langmuir and Freundlich models. The removal of NO_3-N by BC 1&2, and CRH 1&2 can be best modeled using Langmuir isotherm that gave them maximum uptake capacities of 2.380, 1.988, 0.806, and 2.04 mg NO_3-N/g. The results indicate that both materials show potential for adsorption of nitrate-nitrogen.

Keywords: nitrate-nitrogen, adsorption, bamboo charcoal, carbonized rice husk

CMPSD-30

ON THE POWERGRAPH OF A SET

John Mark W. Akut, John Benedict T. Ayawan, Kimberly Hazel B. Camino* and Rosalio G. Artes, Jr.

Department of Mathematics, College of Science and Mathematics
Mindanao State University -Iligan Institute of Technology
Andres Bonifacio Avenue, Tibanga, 9200, Iligan City
*E-mail: misyr_khbc@yahoo.com.ph

Let S be a set. The powerset of a set, denoted by $\wp(S)$, is the set of all subsets of S. A graph is a set of vertices together with the set of edges formed by connecting two vertices. We define the powergraph of S, denoted by $G(\wp(S))$, as the graph obtained from $\wp(S)$ by taking every element of $\wp(S)$ as vertices in and where two vertices x and y in $G(\wp(S))$ are adjacent if and only if the sets corresponding to these vertices have a non-empty intersection.

In this paper, we have characterized all sets which have empty powergraph. Furthermore, we have determined that for a set which contains no element, its corresponding powergraph is a complete graph of order one. We have established that a powergraph of any set S contains a vertex v such that its degree is zero. It is also shown in this paper that for a set containing more than two elements, the size of its powergraph is greater than its order. Among the different observations, we also verified some properties of the vertices corresponding to subsets with different number of elements with respect to the degree. In addition, results on the order of powergraph involving the number of elements of subset S^* are also generated. Lastly, among others, we also investigated some of the properties of graphs induced by the powerset of a given set.

Keywords: set, powerset, powergraph

CMPSD-31

ISOMORPHISM OF SET SYSTEM

Aldever C. Calvo, Jen Roy B. Cruz*, Julie Ann Vanessa P. Chua, and Rosalio G. Artes, Jr.

Department of Mathematics, College of Science and Mathematics
Mindanao State University – Iligan Institute of Technology
Andres Bonifacio Avenue, Tibanga, Iligan City 9200
*E-mail: xtreme2roy@yahoo.com

Mathematics deals with statements concerning objects and the relation between them. Standard mathematical procedure is to identify relations in terms of sets: a relation is a set of objects of a particular kind. In this paper, we will exploit the idea about the isomorphism of set systems. If an isomorphism can be found from a relatively unfamiliar part of mathematics into well studied division of mathematics, where various theorems are already proven, and many methods already exist to find answers, then the function can be used to map problems out of ambiguity over to familiarity where the problem is easier to comprehend.

Isomorphism is studied in mathematics in order to extend insights from one occurrence to another: if two objects are isomorphic, then any property which is preserved by an isomorphism and which is true of one of the objects is also true of the other. When a particularly simple bijection between two sets has been specified, it is sometimes possible to view an object in the domain and its image in the range as virtually indistinguishable: one may be seen as a renaming or a way of rewriting the other. For example, singleton sets and ordered 1-tuples are, strictly speaking, different, but not much harm is done if we occasionally blur the distinction, because of the obvious bijection f such that $f(\{a\}) = (a)$ for any singleton $\{a\}$. Moreover, we have generated results on the isomorphism of set system and presented various examples to further support our assertion. In conclusion, isomorphism is a very useful mathematical resource to aid our venture towards mathematical excellence.

Keywords: Isomorphism, bijection, singleton, 1-tuples

CMPSD-32

ON THE RATIONAL WEIGHT OF AN OPEN SET

Juniel Victor T. Generalao, Eleazar O. Pepito, Euler Yoland B. Guerrero* and Rosalio G.Artes, Jr.

Department of Mathematics, College of Science and Mathematics
Mindanao State University -Iligan Institute of Technology

Andres Bonifacio Avenue, Tibanga, 9200, Iligan City
*E-mail: misyr_geyb@yahoo.com.ph

Given a topological space (U,τ) where the cardinality of U is n, we define the rational weight of an element a of an open set A, denoted by $\omega(a)$ as the image of a under the mapping: $\omega : U \to [0,+\infty)$ given by $\omega(a) = \frac{S_a}{|U|} = \frac{S_a}{n}$

where S_a is the number of sets containing a. For each open set A, we define the rational weight of A as its image of A under the mapping $\Omega : T \to [0,+\infty)$ where $\Omega(A) = \sum_{a \in A} \omega_a$

In this paper, we determined the rational weights involving the basic set operations such as union, intersection, difference, complement, and operations on comparable sets with the notions of topological properties of open sets. Moreover, we have characterized all open sets with rational weight equal to $\frac{2^{n-1}}{n}$ and those with rational weight equal to 2^{n-1} for each $n \geq 1$.

Keywords: rational weight, set, cardinality, mapping, topological space

CMPSD-33

The r – COMBINATORIAL SUBSET AND THE r – COMPLEMENTARY UNION OF SETS

Mhelmar A. Labendia*, Marinel A. Tingcang and Rosalio Artes Jr.

Department of Mathematics
College of Science and Mathematics
MSU- Iligan Institute of Technology
9200 Iligan City
Email: mhelmarlabendia@yahoo.com

This study introduces the unique r – element subset(s) of a finite set in which the sequence of cardinalities follows from the binomial coefficients. It is an endeavour of this paper to give similarities and unusual properties that distinguishes it from the usual set. This study also presents a generalization of

inclusion and exclusion principle, the r – element inclusion and exclusion principle.

The existence of some elements which can be found from the r – element subsets of the union of nonempty finite sets which cannot be found in the union of r – element subsets for every nonempty finite set triggers the researchers to extend the field of set theory especially in the concentration of cardinalities. For these reason, the researchers establish an r – element universal set which is the best tool in finding the complement of every r – element subset. Moreover, the De' Morgans theorem, the subset property, and the intersection property satisfy under this field.

Consequently, the researchers aim to show that this extension could give a generalization of every principle in the usual set. Hence, the researchers also aim to give significant principle even in the field of combinatorics. Specifically, the inclusion and exclusion principle could be extended into an r – element inclusion and exclusion principle since the 1 – element subset follows the usual principle. If r > 1, then we use the r – element inclusion and exclusion principle generated from the combinatorial subsets, the r – element subsets of a set.

Keywords: r-combinatorial subset, r-universal set, complement of r-combinatorial subset, r-complementary union of sets

CMPSD-34

ACCESSIBILITY NUMBER OF SETS

Mary Joy F. Luga*, Ken Rothwyn M. Mira, Aubrey S. Polito and Rosalio G. Artes, Jr.

Department of Mathematics, College of Science and Mathematics
Mindanao State University- Iligan Institute of Technology
Andres Bonifacio Ave., Tibanga, 9200 Iligan City
*E-mail: misyr_mjfl@yahoo.com

Let A and B be finite sets. The distance $d(a,b)$ between two sets A and B is given by $d(a,b) = \min\{ d(a,b): a\in A, b\in B\}$. A set is said to be *k-accessible* from set B if for every $a\in A$, there exists a $b\in B$ such that $d(a,b)\leq k$. The accessibility number of sets from A is given by

$$\delta acc(A,B) = min\{ d(a,b): a\in A, b\in B \}.$$

If A is an empty set, then we say that $\delta acc(A,B) = +\infty$. Given those special subsets of R, we define the most accessible set to A as the set with the least distance to A or the set with the least accessibility number among those given sets. And we define the set with accessibility number equal to positive infinity as the farthest set from A, given that A is the reference set given.

In this study, we provided necessary and sufficient conditions for a set A to have an accessibility number equal to some nonnegative integer. We have also established results on the accessibility number of special subsets of R.

Keywords: accessibility number, sets, absolute difference, distance, k-accessible

CMPSD-35

BINARY OPERATION ON ISOMORPHIC SETS

Jupiter Pilongo* and Kristy Mae Caparida

Department of Mathematics, College of Science and Mathematics
Mindanao State University – Iligan Institute of Technology
Andres Bonifacio Avenue, Tibanga, 9200 Iligan City
*E-mail: pit_wizard0916@yahoo.com

Given two sets $A=\{a_1,a_2,...,a_n\}$ and $B=\{b_1,b_2,...,b_n\}$ where $n\in N$ such $a_i \le a_{i+1}$ and $b_j < b_{j+1}$. We say that A and B are homomorphic if for all $a_i's$, $b_j's$ such that $a_i \neq b_j$, $\forall\, i,j \in N$, $A\cap B=\phi$. Furthermore, two sets are said to be isomorphic if and only if the two sets A and B holds the homomorphism property of two sets and these sets hold the same properties of a sequence. We define the binary operation of a set as

$$A+B=\{a_1+b_1,a_2+b_2,...,a_n+b_n\} \quad \forall n\in \mathrm{N} \ ;$$

$$A\cdot B=\{a_1b_1,a_2b_2,...,a_nb_n\} \quad \forall n\in \mathrm{N} \ ;$$

$$\frac{A}{B}=\left\{\frac{a_n}{b_n},\frac{a_{n-1}}{b_{n-1}},...,\frac{a_1}{b_1}\right\} \quad \forall n\in \mathrm{N} \ ;$$

We have shown in this study that the binary operations such as addition, subtraction, multiplication, and division of two isomorphic sets exist. In addition, the sets $A=\{a_1,a_2,...,a_n\}$ and $\frac{1}{A}=\left\{\frac{1}{a_n},\frac{1}{a_{n-1}},...,\frac{1}{a_1}\right\}$ are isomorphic sets. Moreover, we have established important results on these binary set operations.

Keywords: homomorphism, isomorphism, binary operation, set

CMPSD-36

ON SOME RESULTS OF THE TORSION-FREE ABELIAN TRACE AND KERNEL GROUPS

Jocelyn S. Paradero-Vilela[1] and Ricky B. Villeta[2]

[1]Department of Mathematics, College of Science and Mathematics
MSU-Iligan Institute of Technology
Iligan City, Philippines
Email: csm-jpv@sulat.msuiit.edu.ph
[2]Department of Mathematics, University of San Jose de Recolitos
Cebu City, Philippines

A subgroup K of a group G is said to be *pure* in G (denoted $K \ . \ G$), if whenever $ny \ K$ for some $n \ Z^{+}$ and $y \ G$, then $y \ K$. Equivalently, K is pure in G if and only if $K \ nG = nK$ for all $n \ Z^{+}$.

For any torsion-free abelian groups G and H, the *pure trace* of H in G is defined to be $tr(H,G) = \left\{ g \in G : ng \in \left\langle \sum f(H), f \in Hom(H,G) \right\rangle \text{ for some } n \in Z^{+} \right\}$ and the *kernel* of H in G is defined to be $\ker(G,H) = \bigcap_{f \in Hom(H,G)} \ker f$. The pure trace and kernel of H in G are pure fully invariant subgroups of G.

Two classes of groups emerged from these classes of pure fully invariant subgroups. A torsion-free abelian group G is said to be a *trace group* if for every pure fully invariant subgroup M of G, $M = tr(M,G)$ and G is said to be a *kernel group* if $M = ker(G,G/M)$ for every pure fully invariant subgroup M of G.

The groups of integers and rational numbers are both trace and kernel groups. More generally, since an irreducible group is a group having no proper pure fully invariant subgroups, it is then a trace and kernel group. Hence, the strongly irreducible groups which are known to be irreducible, are also trace and kernel groups. It is important to note that in the literature, the class of strongly irreducible groups serves as the very foundation or building blocks in the classification of torsion-free abelian groups.

This paper proves the properties of the trace and kernel groups in relation to the direct summands and direct sum of groups.

Keywords: trace groups, kernel groups, pure fully invariant subgroups, irreducible groups, strongly irreducible groups.

CMPSD-37

ON THE *k*-SUBGRAPHS OF THE GENERALIZED HYPERCUBES

Geoffrey A. Solano[1] and Jaime D.L. Caro[2]

[1]Department of Physical Sciences and Mathematics
University of the Philippines-Manila, Philippines
E-mail: gasolano@up.edu.ph
[2]Department of Computer Science
University of the Philippines-Diliman, Philippines
E-mail: jdlcaro@gmail.com

Graphs are used in modeling interconnections networks and measuring their properties. Knowing and understanding the graph theoretical/combinatorial properties of the underlying networks are necessary in developing more efficient parallel algorithms as well as fault-tolerant communication/routing algorithms.

The hypercube is one of the most versatile and efficient networks yet discovered for parallel computation. One generalization of the hypercube is the n-cube $Q(n,m)$ which is a graph whose vertices are all the binary n-tuples, such that two vertices are adjacent whenever they differ in exactly m coordinates. The k-subgraph of the Generalized n-cube $Q_k(n,m)$ is the induced subgraph of the n-cube $Q(n,m)$ where $q=2$, such that a vertex v $V(Q_k(n,m))$ if and only if v $V(Q(n,m))$ and v is of parity k.

This paper presents some degree properties of $Q_k(n,m)$ as well as some isomorphisms it has with other graphs, namely:

1) $Q_{n-1}(n,2)$ is isomorphic to Kn
2) $Q_k(n,2i)$ is isomorphic to $G_i(n,k)$
3) $Q_n(n,2i)$ is isomorphic to $SG_i(n)$

Keywords: graphs, hypercubes, networks, parity, graph properties

CMPSD-38

CONVEX ACCESSIBILITY OF GRAPHS

Randy L. Caga-anan* and Rosalio G. Artes, Jr.

Department of Mathematics, College of Science and Mathematics
Mindanao State University - Iligan Institute of Technology
Andres Bonifacio Avenue, Tibanga, 9200 Iligan City
*E-mail: ranlica@yahoo.com

This study endeavored to help solve some current and future energy allocation problems which can be modeled by a particular notion in graph theory studied in this paper.

Given a connected graph G, we define the distance $d_G(u,v)$ between two vertices u and v in G as the length of a shortest path joining u and v in G. A subset S of $V(G)$ is said to be convex if for every pair of vertices u and v in S, the vertices of any u-v shortest path lie entirely in S. A graph G is said to be convex k-accessible if G contains a proper convex set S such that for every $v \in V(G)$, $d_G(u,v) \leq k$ for some $u \in S$. The convex accessibility number of G is given by $con_a(G) = \min\{k : G \text{ is a convex } k\text{-accessible graph}\}$.

This paper combined the concept of convexity borrowed from analysis and the notion of accessibility in graph theory. For a positive number $k \geq 1$, it is shown that there exists a graph G of convex accessibility number exactly equal to k. The construction of such a graph is then given. Moreover, it characterized all graphs having convex accessibility number equal to 1. Finally, it established results on the convex accessibility number of path, cycle, wheel, fan, complete graph, complete bipartite graph, and graphs resulting from some binary graph operations.

Keywords: convex, accessibility, proper, k-accessible, distance

CMPSD-39

ON THE BUNDLE NUMBERS OF GRAPHS

Genyluz M. Dangin, Euler Yoland B. Guerrero and Romulo C. Guerrero*

Department of Mathematics
College of Science and Mathematics
MSU-Iligan Institute of Technology
Iligan City, 9200
E-mail: romy1325@yahoo.com

A *clique* is a set of pairwise adjacent vertices in a graph G. We denote by C(G) and c(G), to be the set of cliques and the cardinality of C(G), respectively. We shall call c(G) the *bundle number* of G. Let $C_k(G)$ be the set of k-cliques in G. Then the number of k-cliques in G denoted by $c_k(G)$ is the order of $C_k(G)$, that is, $c_k(G) = |C_k(G)|$. This paper is a research in Graph Theory which uses both simple counting techniques and sophisticated combinatorial arguments in computing the number of cliques in a graph. Results involving the bundle numbers of some special graphs like trees, cycles, complete bipartite graphs, corona of two graphs, and union of graphs are presented.

Specifically, this study generated among others the following results:

1. Given a graph G with the clique number $\omega(G)$. Then $C(G) \subseteq \bigcup_{k=0}^{\omega(G)} C_k(G)$ and so $c(G) = \bigcup_{k=0}^{\omega(G)} c_k(G)$
2. Let G. be a graph with $V(G) = \{v_1, v_2, ..., v_n\}$. Then the number of k-cliques in G is at most $\binom{n}{k}$. That is, $c_k(G) \le \binom{n}{k}$ and $c(G) \le \sum_{k=0}^{n} \binom{n}{k} = 2^n$.
3. $c(G+H) \ge c(G) + c(H)$ for two graphs G and H.
4. Let G and H be graphs. Then $c(G \circ H) = c(G) + |G|[c(H + v_i) - 2]$, $v_i \in V(G)$
5. Given $p>0$, there exists a graph G. not necessarily unique, such that c(G) = p.

Lastly, this study has discovered some practical applications to business, economics, and organizational studies. For instance, in business and economics, the bigger the bundle number the better is the condition of the business.

Keywords: clique, cardinality, bundle number,corona

CMPSD-40

FOLDING BIPARTITE GRAPHS AND THE SUM OF GRAPHS

Severino V. Gervacio[1] and Romulo C. Guerrero[2]

[1]Department of Mathematics
De La Salle University, 2401 Taft Avenue, 1004 Manila
E-mail: gervacios@dlsu.edu.ph
[2]Department of Mathematics
MSU-Iligan Institute of Technology, Tibanga, Iligan City 9200
E-mail: romy1325@yahoo.com

If two non-adjacent vertices of a connected non-complete graph G that have a common neighbor are identified and the resulting multiple edges are reduced to simple edges, then we obtain another connected graph of order one less than that of the original graph. If a similar process is applied to the new graph, and we repeat the

operation until there are no more non-adjacent vertices, we finally get a complete graph. We say that the graph is folded into a complete graph. We denote by $F(G)$, called the fold of G, the set of all complete graphs, up to isomorphism, into which a graph G can be folded. Among others, this study characterizes the graphs that folds into the complete graph K_2 and shows that the fold of the sum of a finite number of graphs is equal to the sum of the folds of the graphs.

This study came up with the following results:

1. $F(G)=K_2$ if and only if G is a (connected) bipartite graph.
2. (a) $K_{\chi(G)}$ is the smallest folding of a graph G, where $\chi(G)$ is the chromatic number of G.
   (b) $\chi(G + H) = \chi(G) + \chi(H)$, for any two connected graphs G and H.
3. (a) $F(G + H) = F(G) + F(H)$, for any two graphs G and H.
   (b) $F(\sum_{i=1}^{n} G_i) = \sum_{i=1}^{n} F(G_i)$, for all graphs G_i, $i = 1,2, \ldots, n$.
4. (a) $F(G + H) = K_4$ if and only if G and H are bipartite graphs.
   (b) $F(\sum_{i=1}^{n} G_i) =$ if and only if G_i is a bipartite graph i, $i = 1, \ldots, n$.

Keywords: fold of a graph, complete graph, sum of graphs, bipartite, chromatic number

CMPSD-41

EDGE-MONOPHONIC NUMBER OF THE JOIN OF GRAPHS

Alexis Bernard A. Dalam[1*] and Rowena T. Isla[2]

[1]Mathematics Department, Jose Rizal Memorial State College, Dapitan City
Tel.: (065)213-6444; *E-mail: ab_dalam@yahoo.com
[2]Mathematics Department, MSU-Iligan Institute of Technology, Iligan City
Telefax: (063)221-4068; E-mail: rt_isla@yahoo.com

A subset $S \subseteq V(G)$ of a graph G is an *edge-monophonic set* of G if every edge of G lies on some monophonic or chordless path joining two vertices of S. The *edge-monophonic number* of G, denoted by *enm (G)*, is the minimum cardinality of an edge-monophonic set of G. This study characterizes edge-monophonic sets in the join of graphs and gives the edge-monophonic number of such graphs.

Keywords: edge-monophonic, chordless path, cardiality

CMPSD-42

ON THE LINEAR SUM OF GRAPHS

Joselito A. Uy[1]*, Rowena T. Isla[1] and Teresa L. Tacbobo[2]

[1]Department of Mathematics, MSU-Iligan Institute of Technology, Iligan City
Tel.: (063)221-4050 loc 140; Fax No. (063)221-4068;
E-mail: csm-jau@sulat.msuiit.edu.ph
[2]Mathematics Division, Bukidnon State University, Malaybalay City

A linear labeling of a graph G is a one-to-one mapping from the vertex set of G into the set $\{1, 2, \ldots, n\}$. The linear sum of linear labeling f of G is $\Sigma\,|f(u) - f(u)|$, where the sum is taken over all edges uv in G. The linear sum $s(G)$ of G is the minimum of all linear sums of linear labelings of G. This paper investigated the linear sum of graphs resulting from graph operations. Let v and e be a vertex and an edge, respectively, of complete graph K_n. For any n, $s(K_n - e) = (n^3 - 7n + 6)/6$. If $n \geq 2$, then $s(G) = n(n-1)(n-2)/6$. Graph operations particularly considered were cartesian product, edge and vertex deletion, closure, line graph, and complement.

Keywords: linear labeling, linear sum of labeling, linear sum of graph

CMPSD-43

DERIVATIVE OF A CONTINUOUS GRAPH VIA ITS DEGREE SEQUENCE POLYNOMIAL REPRESENTATION

Joan B. Ybañez* and Rosalio G. Artes, Jr.

Department of Mathematics, College of Science and Mathematics
Mindanao State University - Iligan Institute of Technology
Andres Bonifacio Avenue, Tibanga, 9200 Iligan City
*E-mail: misyr_jby@yahoo.com.ph

A non-empty graph G is said to be continuous if every pair of vertices x and y in G are joined by a path. In a continuous graph G, the degree of a vertex v is the number of edges incident with v in G. The degree sequence polynomial representation of a graph G is the polynomial of the form $f_G(x) = \sum_{i=0}^{k} a_i x^i$, where a_i is the number of vertices in G with degree i from this representation, we define the derivative of the degree sequence polynomial as $f'_G(x) = \sum_{i=1}^{k} i a_i x^{i-1}$

A continuous graph G is also said to be semi-differentiable if and only if there exists a graph G' such that $f'_G(x) = f_{G'}(x)$. A graph G', if it exists, is a semi-derivative of G. A semi-differentiable graph is said to be differentiable if G' is unique. In this case, G' is the derivative of G.

In this paper, we established some basic properties of the derivative of a continuous graph via its degree sequence polynomial representation. We also determined the derivative of some special graphs such as path, cycle, fan, wheel, complete graph, and complete bipartite graph. Furthermore, the derivative of graphs resulting from the join and the corona of graphs are also generated. Moreover, we have shown that for positive integer n, there exists a differentiable graph of order n. Further, we have generated a result that if a graph G is 3-regular, then G admits a unique continuous derivative.

Keywords: derivative, continuous graph, degree sequence polynomial representation

CMPSD-44

DOMINATING SET AND DOMINATING NUMBER OVER A COLLECTION

Joan B. Ybañez*, Mary Kris Remulta, Toni Rose C. Herrera and Rosalio G. Artes, Jr.

Department of Mathematics, College of Science and Mathematics
Mindanao State University - Iligan Institute of Technology
Andres Bonifacio Avenue, Tibanga, 9200 Iligan City
*E-mail: misyr_jby@yahoo.com.ph

Let X be a non-empty set and be a collection of subsets of X. A subset $A \in \Omega$ is said to *dominate* $B \in \Omega$ if $A \cap B \neq \emptyset$ and $|A \cap B| \geq |A \cap C|$ for any $C \in \Omega$. The *dominating number of A over* Ω, denoted by $dom_{X,\Omega}(A)$, is the number of subsets of X in Ω which are dominated by A. If Ω_1 is the subcollection of containing all the subsets of X dominated by A, the $dom_{X,\Omega}(A) = |\Omega_1|$.

We have characterized all subsets of X which have dominating number over Ω equal to some non-negative integers. A non-empty set X is said to dominate every element of Ω. Hence $dom_{X,\Omega}(X) = |\Omega|$, whenever $X \notin \Omega$. In addition, we have shown that for any A subset of B, the dominating number of A over Ω.

In this study, we established some basic properties of the dominating number of a set over a collection. We also determined some important existent theorems and behavior of the dominating number over a collection of subsets of a non-empty set X.

Keywords: cardinality, dominating set, dominating number, collection of subsets, subcollection

CMPSD-45

TRAINING-LESS OPTICAL RECOGNITION OF PRINTED CHARACTERS USING EQUATION FITTING

Rev M. Matugas* and Jaderick P. Pabico

Institute of Computer Science
College of Arts and Sciences
University of the Philippines Los Baños, College 4031, Laguna
Tel/Telefax: 63-49-536-2313/63-49-536-2302
Email: matugas.rev@gmail.com

We present a novel computational method for optical recognition of printed characters based on our observation that a character image can be divided into several partitions, where each represents a simple mathematical equation. In this paper, we derived a set of mathematical equations to respectively fit parts of an alphanumeric character. Using these equations in tandem with digital image processing, we can identify characters without going through tedious supervised machine training sequences where large samples of learning patterns is required. We digitized ten samples each of printed alphanumeric characters, and store each image in a matrix M, where the (i,j)th matrix element $m_{i,j} = I$. To remove noise, we converted M into binary using a thresholding value h, setting all $m_{i,j} > h$ to 1, and to 0 otherwise. We "thinned" M by reducing to 0 some matrix elements in the Moore neighborhood of a chosen $m_{i,j} = 1$, following the Rutovitz and Hilditch thinning procedures, to make sure that a continuous thin line is visible in M. We divided the thinned M into six partitions: two columns and three rows. In each partition, we extracted the coordinates (i,j) of each $m_{i,j}=1$ and subjected them to equation fitting.

We determined which equation the image part fits best using a simple correlation analysis. We developed a table of patterns for each character, wherein a table entry that matches the 6-part pattern determines the alphanumeric character. We validated our method using 360 images where our method correctly classified 94% of Arial fonts. Of the 6% error, our method interchangeably identified C as G, 9 as S, and I as T. Based on the promising result from our validation method, we

conclude that our method is a potential alternative optical recognition scheme, specifically on machine printed characters.

Keywords: optical character recognition, training-less, equation fitting.

CMPSD-46

CONSTRAINED MULTIPLE SEQUENCE ALIGNMENT TOOL

Vincent Peter C. Magboo* and Honeylette B de Luna

Department of Physical Sciences and Mathematics,
College of Arts and Sciences
University of the Philippines Manila, Padre Faura, Ermita, Manila
Telefax: 7256717; E-mail: petermagboo@yahoo.com

Constrained Multiple Sequence Alignment provides biologists a way to incorporate their knowledge about the functionalities and structure of sequences in their alignments. It has been anticipated that constrained sequence alignment was to integrate the knowledge of biologists with regards to the structures/functionalities/consensus of their data sets into sequence alignments such that specified residues matching the given constraints are aligned together in the result.

The "Constrained Multiple Sequence Alignment Tool" (CMSA Tool) is an online application which uses the memory-efficient CPSA (Constrained Pairwise Sequence Alignment) algorithm in aligning multiple sequences. Input validation provided by CMSA Tool ensures that the data processed by the server are correct. Sequence input can be done via text files, text area and from the sequence database. The CMSA Tool generates a text file that is available for the user to download. The CMSA Tool Database allows users to browse through the biological sequences, substitution matrices and CMSA results. The tutorial module built within the CMSA Tool allows the lesson administrator to update the text part of the lessons in the database, upload images and supplementary materials important in the understanding of the lessons. The tutorial module also allows users to take an automatically generated test assess their knowledge of the lessons.

Keywords: constrained multiple sequence alignment, memory--efficient, biological sequences, substitution matrices

CMPSD-47

COMBINATORIAL PATTERN DISCOVERY TOOL

Vincent Peter C. Magboo* and April O. Harina

Department of Physical Sciences and Mathematics,
College of Arts and Sciences
University of the Philippines Manila, Padre Faura, Ermita, Manila
Telefax: 7256717; E-mail: petermagboo@yahoo.com

Sequence pattern discovery aims at developing tools and methods for finding a priori unknown patterns in a given set of biological sequences, patterns that are frequent, unexpected or interesting according to some formal criteria. A pattern or a motif is a repeating subsequence and often has a vital biological role.

The Combinatorial Pattern Discovery Tool is a web-based application tool which aims to find the maximal patterns from a given set of protein/DNA/RNA sequences. Maximal patterns are found using the Teiresias algorithm involving two phases: scanning phase and convolution phase. The offset lists corresponding to the maximal patterns, which determine the locations of a specific maximal pattern in the input sequences, are also displayed. The users of the system can browse through each of the maximal patterns and their corresponding offset list and save them in their hard disks. In addition, there is atutorial module which provides lectures and supplementary materials to aid in the understanding of concepts behind the discovery of patterns in biological sequences. A Flash animation file is also included to demonstrate how the Teiresias algorithm wortks given a sample input. An automatically generated test is also provided to test the users about maximal patterns. Teiresias algorithm does not enumerate the entire solution space, thus saving a considerable amount of time. The reported patterns generated possess the maximality property and cannot be made more specific without simultaneously reducing the size of its offset list. However, it requires significant amount of memory to perform its task.

Finding the maximal patterns found in biological sequences is important for molecular biologists as these usually corresponds to residues conserved during the evolution due to an important structure or functional role.

Keywords: maximal patterns, biological sequences, sequence similarity, Teiresias algorithm

CMPSD-48

MSA: MULTIPLE SEQUENCE ALIGNMENT

Ma. Sheila A. Magboo

Department of Physical Sciences and Mathematics,
College of Arts and Sciences,
University of the Philippines Manila, Padre Faura, Ermita, Manila
Telefax: 5265858; E-mail: sheilaabad@yahoo.com

MSA: Multiple Sequence Alignment is a web-based tool capable of aligning three or more biological sequences which can either be DNA, RNA, or protein. In general, the input set of query sequences are assumed to have an evolutionary relationship by which they share a lineage and are descended from a common ancestor. From the resulting MSA, sequence homology can be inferred and phylogenetic analysis can be conducted to assess the sequences' shared evolutionary origins.

MSAs require more sophisticated methodologies than pairwise alignment because they are more computationally complex to produce. Most multiple sequence alignment programs use heuristic methods rather than global optimization because identifying the optimal alignment between more than a few sequences of moderate length is prohibitively computationally expensive.

This MSA project was patterned after ClustalW and hence employs heuristics to find a good multiple sequence alignment. It starts by doing pairwise alignment between sequences to determine the degree of similarity between each pair. The result of this alignment is stored in a distance matrix. The second step involves the construction of a similarity tree using the distance matrix and the Neighbor-Joining method wherein the root is placed at the midpoint of the longest chain of consecutive edges. The last step involves the combination of the alignments starting from the most closely related groups to the most distantly related groups by going from tip of tree to the root of the tree.

This MSA project can accept sequences with the following format: NBRF / PIR, EMBL / UniProtKB/ Swiss-Prot, Pearson (Fasta), GDE, ALN / ClustalW, GCG / MSF, RSF. The user can adjust a number of parameters such as the gap and pag-extension penalties.

Keywords: multiple sequence alignment, phylogenetics, ClustalW

CMPSD-49

A JOHNSON SCHEME INTERPRETATION OF NUCLEOTIDE ALPHABET COMPOSITION

Geoffrey A. Solano[1] and Jaime D.L. Caro[2]

[1]Department of Physical Sciences and Mathematics
University of the Philippines-Manila, Philippines
E-mail: gasolano@up.edu.ph
[2]Department of Computer Science
University of the Philippines-Diliman, Philippines
E-mail: jdlcaro@gmail.com

The purine-pyrimidine and hydrogen donor-acceptor pattern governing nucleotide recognition have been shown to correspond formally to a digital error-detecting(parity) code when the said properties are used to give each informationally distinct nucleotide a unique 4-bit numerical representation. The potential nucleotide alphabet of 16 letters corresponds to the set of all 16 4-bit numbers (the binary space B^4). McDonnail has shown that nucleotide, so interpreted, may be depicted as positions on a hypercube Q_4. By introducing a mapping (v) = v', of $v=a_1a_2a_3 \ldots a_nQ_4$ into a set v' such that j v' if and only if $a_j = 1$. The set of all resulting v's will yield the power set 2^A where A= {1,2,3,4}, which can be expressed as vertices of the ith graphs of the Johnson Scheme $G_i(n,k)$ for k=0...4. We note that a particular ith graph of the Johnson Scheme $G_2(4,2)$ is a graph where two vertices are adjacent if they are base pairs.

It has already been suggested before that factors other than physiochemical issues alone shaped the natural nucleotide alphabet. This paper shows that such shaping as well as the interrelationships of the nucleotide alphabet are supported by the theory of association schemes.

Keywords: DNA, parity, association schemes, johnson scheme, nucleotide

CMPSD-50

ELECTRICAL CHARACTERISTICS OF AMORPHOUS ZnO FOR UV SENSORS APPLICATION

Jess E. Gambe* and Reynaldo M. Vequizo

Materials Science Laboratory, Department of Physics,
Mindanao State University – Iligan Institute of Technology,
Andres Bonifacio Avenue, Iligan City 9200, Philippines,
Email: dives2003@yahoo.com*, reyvequizo@yahoo.com

Active materials of UV detectors such as single crystalline ZnO, are capable to convert electromagnetic energy to current and are commonly grown in vacuum condition which is expensive. In this study, we introduce an amorphous ZnO having 99.0% purity as an alternative semiconductor for photodetectors using Metal-Semiconductor-Metal (MSM) configuration via point and interlocking electrode configurations. The preparation and characterization were done in a non-vacuum condition which is economical. The ZnO powders were dried at 200, 300 and 400°C for 1 hour and were then pelletized at 8 tons for 2 minutes/sample. The electrical characteristics of the samples were measured using the Van der Pauw technique and results show the resistivity of the dried samples decreases about 10 times lower than that of the undried and as-prepared samples which could be due to the removal of moisture after drying. All samples exhibit n-type behavior and the conductivities (10^{-7}-10^{-5}S/cm) of the samples increase with higher temperature. In comparison to a single crystal ZnO grown using hydrothermal method, the carrier concentrations of the samples are low n-type (10^{10}-10^{11}cm^{-3}) material. No significant change of the Hall factor of the samples is observed; but it is 100,000 times lower than the reported ZnO single crystal. The Hall mobility is of the order 10^{4}-10^{5}cm^{2}/V·s which is large and investigations are undergoing for further clarification.

The current-voltage curves for samples with the point electrode configuration under UV illumination (365nm) using two-probe technique show significant change in the conductivity about 10-10,000 times that of the dark condition. For the current-voltage curves of the samples with interlocking electrode MSM configuration exhibits the same behavior of increasing conductivity under UV illumination, but the increase is about 10 times that of its dark condition. These findings show the potential of amorphous ZnO for UV sensing.

Keywords: photodetector, ZnO, metal-semiconductor-metal, Van der Pauw technique

CMPSD-51

GERMICIDAL LAMP-INDUCED SYNTHESIS OF SILVER NANOPARTICLES IN CROSSLINKED POLYMER GLOBULES

Concepcion Ponce*, Emee Grace Tabares, Raul Olaguer

[1]Division of Physical Sciences and Mathematics, UP Visayas,
Miag-ao, Iloilo 5023
Telefax: (033) 513-7020; *Email: concepcion_ponce@yahoo.com*

A lot of photochemical methods for synthesizing nanoparticles have been presented in literature already but they involve expensive materials and equipment like the use of high pressure mercury lamp under nitrogen atmosphere. This study presents a very simple and cheap method of generating nanoparticles stabilized

by a crosslinked polymer globule. The process involves the addition of varying amount of silver nitrate into a 1 mg/mL aqueous solution of polyacylic acid (PAA) and irradiating the sample using four 10-watt UVC germicidal lamps in open air vessels.

Polyacrylic acid assumes a coiled conformation in its unionized from and an extended conformation in its ionized form. Addition of silver ions collapses the PAA chains into globules. Irradiation crosslinks the PAA chains and makes the globular structure as verified by kinematic viscosity studies. The viscosity of the original silver ions/PAA solution was 1.057 centipoise. Titrating it with sodium hydroxide caused the viscosity of the unirradiated solution to increase to 961.1 cP while that of the irradiated solution increased only slightly to 1.292 cP. This difference indicates that the silver-PAA complex retained its globular structure and resist large conformational changes after the irradiation process.

Increasing the radiation exposure not only crosslinks the PAA but also reduces the silver ions into the metallic state. UV-Vis spectra of the solutions showed the characteristic plasmon absorbance of silver nanoparticles at 440 nm and the AgPAA complex absorbance at around 800 nm. Scanning electron micrographs of the silver-PAA complex showed the particles synthesized using this method have sizes ranging from 50-300 nm.

Keywords: crosslinked polymer globules, silver nanoparticles, UVC germicidal lamp radiation

CMPSD-52

SURFACE MORPHOLOGY OF POLYANISIDINE-POLYVINYL ACETATE COMPOSITE FILMS

Francis Murillo Emralino* and Marvin Ustaris Herrera

Materials Physics Research Laboratory
Physics Division, Institute of Mathematical Sciences and Physics
University of the Philippines - Los Baños
C-203 Physical Sciences Building, UPLB, College, Laguna 4031
Tel.: (049) 536-1841, Fax: (049) 536-6610
*E-mail: francis_emralino@yahoo.com, muherrera@yahoo.com

Fabrication of polyanisidine (PAnis) composite films using five different concentrations of polyvinyl acetate (PVA) was successfully carried out. In this present study, we aim to investigate the possibility of film formation through the use of PVA, a synthetic polymer determined to contain a functional additive called plasticizer which accounts for the flexibility associated with its use. Morphological investigations on the films were facilitated using a Hitachi TM-1000 Tabletop scanning electron microscope.

Standard oxidative polymerization was used in the synthesis of our Polyanisidine samples. Perchloric acid was used as the dopant since theoretical and experimental results attest for its ability to increase the samples' conductivity.

Formation of the films was done by combining five different concentrations of PVA with the polyanisidine samples. The amount of PAnis was set to a constant mass for each sample. Each of these mixtures was then uniformly layered onto sensitized film substrates.

We captured images of each of the five fabricated films at 500x magnification from the scanning electron microscope and these were used to look into the morphology of the fabricated films. The images revealed clear mixing of PAnis and binder. At low binder concentration, the films were still coarse with the grains of our PAnis still visible. But with the films of higher binder concentration, smoothening of the film surfaces were now observed.

It can be interpreted that the inclusion of binder in substantial degree of concentration facilitates effective dispersion of the polymer grains into the binder and results to the smoothing of the film surfaces as was observed.

Keywords: polyanisidine, conducting polymer, composite films

CMPSD-53

DIP SELF-ASSEMBLY OF AgPAA-PDDA ON GLASS: INFLUENCE OF IONIC STRENGTH

Concepcion Ponce[1*], Leon M. Payawan[2] and M. Cynthia Goh[3]

[1]Division of Physical Sciences and Mathematics, UP Visayas,
Miag-ao, Iloilo 5023
[2]Institute of Chemistry, Palma Hall
University of the Philippines Diliman, Quezon City 1101
[3]Department of Chemistry, University of Toronto
80 St. George Street, Toronto, ON Canada, M5S 3H6
Email: concepcion_ponce@yahoo.com

Dip self-assembly is a popular method of fabricating thin films with highly ordered structures and tunable properties. The main attraction of the technique, which is based on alternate deposition of oppositely charged species on a charged surface, is due to the low cost and ease with which functional thin films can be designed. In this study, the method is applied to the preparation of multilayers composed of silver polyacrylate (AgPAA) nanocomposites and polydiallyldimethylammonium chloride (PDDA) on a glass substrate. The salt content of the PDDA solution was varied to study the effect of ionic strength on the deposition of AgPAA on PDDA.

The AgPAA nanocomposites have a net negative charge due to residual carboxylate groups on PAA. In turn, this negative charge allowed the deposition of AgPAA on the surface of a polycation, PDDA. The thickness and surface roughness of the films produced are influenced by ionic strength of the PDDA dipping solution. With no added salt, 5 nm-thin and flat films are produced. Increasing the salt concentration to 0.1 M produced 80 nm-thick and rough films as shown in the atomic force microscopy (AFM) images. This difference is explained by considering the conformational transition from extended chains at low ionic strength to globular coil at high ionic strength of PDDA in solution. However, further increase in salt concentration resulted in thinner films. It is possible that the chloride ions from the added salt effectively competed with AgPAA for positively charged sites and displaced it from the PDDA surface. Thus, for a PDDA/AgPAA polyelectrolyte multilayer system, the best condition for deposition is at 0.1 M NaCl concentration.

Knowing these conditions, one can tailor the thickness and morphology of AgPAA-PDDA thin films and apply it to the fabrication of photonic Bragg-stack structures.

Keywords: dip self-assembly, silver-polyacrylate nanocomposite, polymer multilayers

CMPSD-54

OPTIMAL CONTROL OF THIN FILM FLOW WITH STATE ESTIMATION FROM NOISY MEASUREMENTS

Valentine Blez L. Lampayan[1,2], Christian Victor L. Arellano[1], Jose Ernie C. Lope[1*] and Ricardo C.H. del Rosario[1,3]

[1]Institute of Mathematics
University of the Philippines, Diliman, Quezon City, 1101, Philippines
Tel./Fax : +632-920-1009
[2]Division of Natural Sciences and Mathematics
University of the Philippines in the Visayas, Tacloban College
[3]Max Planck Institute of Biochemistry, Department of Membrane Biochemistry
Am Klopferspitz 18, 82152 Martinsried, Germany
E-mail: Residue117@yahoo.com (C.V.L. Arellano),
ernie@math.upd.edu.ph (J.E.C. Lope),
rcdelros@biochem.mpg.de (R.C.H. del Rosario)

The Kuramoto-Sivashinsky (KS) equation is a (one-dimensional) simplified form of the Navier Stokes equations which is useful in studying certain cases of thin film flow. This equation was first introduced by Kuramoto in the study of phase turbulence in the Belousov-Zhabontinsky reaction and has been useful in a wide range of applications including concentration waves, plasma physics, flame

propagation and viscous flow problems. In this work, we study its applications where the vertical flow of a thin film is desired to have as small fluctuations as possible, e.g., in applications where a certain material lying horizontally on a conveyor belt is coated with a film flowing vertically.

Let $z \in \Omega = [-\pi, \pi]$ denote the vertical axis, and let $\eta(z,t)$ denote the distance of the film from the vertical plane. The KS equation is given by

$$\frac{\partial \eta(z,t)}{\partial t} + \frac{\partial^4 \eta(z,t)}{\partial z^4} + \frac{\partial^2 \eta(z,t)}{\partial z^2} + \eta \frac{\partial \eta(z,t)}{\partial z} = 0 \tag{1}$$

with initial condition $\eta(z,0) = \eta_0(z)$ (2)

and periodic boundary conditions $\frac{\partial^n \eta(-\pi,t)}{\partial z^n} = \frac{\partial^n \eta(\pi,t)}{\partial z^n}, n = 0,1,2,3.$ (3)

The displacement η is not measured at all points along the vertical surface, and typically, one or two point sensors along the wall are employed. Thus, the full displacements (or the full state of the system) must be reconstructed from one or two point observations. Furthermore, these measurements are corrupted by noise and hence we will consider measurements with white Gaussian noise. By employing appropriate approximation methods (i.e., choosing basis functions which satisfy the boundary conditions (2) and which satisfy the necessary smoothness requirements), then the finite-dimensional (in space) KS equation can be written in the form

$$M\dot{x}(t) + Ax(t) + N(x(t)) = Bu(t) + w(t), x(0) = x_0$$
$$y(t) = Cx(t) + v(t). \tag{4}$$

Here x is the state vector, u is the control vector, w is the system noise, C is the state observation operator, y is the noise-corrupted state measurements, and the function N contains the non-linear components of the model.

The Linear Quadratic Gaussian (LQG) Problem is to minimize the performance index

$$\min J(u(t)) = \lim_{T \to \infty} \frac{1}{T} E\left\{ \frac{1}{2} \int_0^\infty \left[x^T(t) Q x(t) + u^T(t) R u(t) \right] dt \right\} \tag{5}$$

subject to (4).

By solving the LQG problem, we obtain the optimal control in feedback form. We present our numerical results in Figures 1, 2, and 3. Figure 1 shows the true state of the uncontrolled system, Figure 2 is the controlled system using linear control and partial state observation (with a point measurements at z=pi/2) and Figure 2 is the controlled system using LQG feedback control.

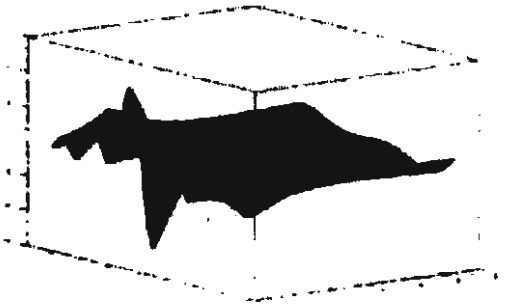

Figure : The uncontrolled system

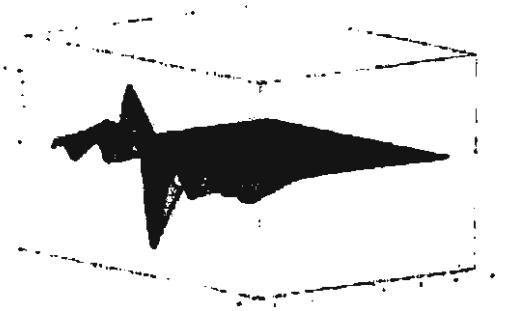

Figure : Controlled system using linear control and state reconstruction

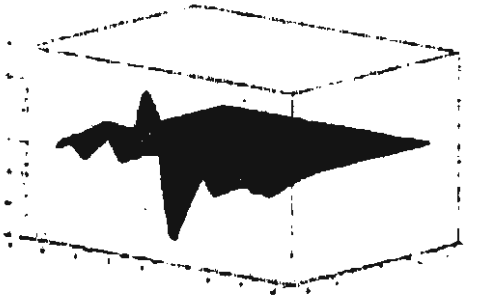

Figure : Controlled system using LQG optimal control with state reconstruction

Keywords: LQG Control, state estimation, optimal feedback control, Kuramoto Sivashinsky equations, thin film flow

CMPSD-55

SURFACE MORPHOLOGY OF BI-2212 FILMS GROWN BY PULSED LASER DEPOSITION

J. C. de Vero*[1], J. F. Gabayno[1], W.O. Garcia[2] and R. V. Sarmago[1]

[1]Condensed Matter Physics Lab., National Institute of Physics
[2]Photonics Research Lab., Nat. Inst. of Physics
University of the Philippines Dil., Quezon City 1101
Tel/.Fax: (02)9280296; E-mail: jcdevero@up.edu.ph, jfgabayno@up.edu.ph

Bi-2212 films on MgO substrates were grown via pulsed laser deposition technique. A bulk Bi-2212 superconductor stoichometric target and substrate are mounted inside the vacuum chamber. The target was irradiated with a 1064 nm pulsed Nd: YAG laser with repetition rate of 10 Hz under an atmospheric pressure of 10^{-3} mbar. The films were annealed ex- situ at different duration. A longer annealing time produced better morphological properties, such as growth of more planar grains, smoother surface and more homogenous composition. XRD of longer annealed films also indicated better film crystallinity.

Keywords: surface morphology, stoichometric, planar grains, film crystallinity

CMPSD-56

CALCULATION OF THE WINDING PROBABILITY FOR AN ENTANGLED POLYMER WITH A HARMONICALLY LENGTH VARYING POTENTIAL

Mark Nolan Confesor [1]*, Jinky Bornales[1], Christopher Bernido[2], and M.V. Carpio-Bernido[2]

[1]Department of Physics, College of Science and Mathematics
Mindanao State University – Iligan Institute of Technology,
Andres Bonifacio Ave., Tibanga, Iligan City, 9200 Philippines
*Email: mark@physics.msuiit.edu.ph
[2]Research Center for Theoretical Physics
Central Visayan Institute Foundation, Jagna, Bohol, 6308 Philippines

Recently C.C.Bernido et.al. use the stochastic white noise analysis to solve the polymer entanglement problem for a class of length dependent potentials (C.Bernido, M.V.Carpio-Bernido and J.Bornales 2005,2006,2007).

Their calculations follow the Hida and Streit formulation of the path-integral. The results of their calculations were able to describe some interesting physical characteristics of proteins such as chirality.

In this work we calculate the winding probability of an entangled polymers for a class of harmonically length varying potentials. Moreover we use the procedure developed by Wiegel (Wiegel,1986) wherein the winding probability is solved from a diffusion like equation. Here, we take as an example the case where the potential varies as a periodic cosine of the form

$$W_n(N) \approx \frac{R}{l}\sqrt{\frac{4\pi}{N}}\exp\left\{-\frac{R^2}{Nl^2}\left[2\pi n - \frac{k}{2\alpha R^2}\sin^2(\alpha L)\right]\right\}$$

where R is the winding radius. For $k = 0$ we obtain the result for a random walk in a circle (Wiegel,1983).

Keywords: entanglement, winding probabilities

CMPSD-57

SINGLE BEAM PERFORMANCE TEST FOR THE GLOBAL LARGE DETECTOR CALORIMETER

Filchito Renee G. Bagsican* and Dennis C. Arogancia

Department of Physics, College of Science and Mathematics
Mindanao State University – Iligan Institute of Technology
Andres Bonifacio Ave., Tibanga, Iligan City, 9200 Philippines
*Email: tjbagsican@gmail.com

The International Linear Collider (ILC) is a proposed linear collider that would surpass any other linear colliders of today in terms of center-of-mass collisions. One of the goals of the ILC is to understand the mechanism behind mass generation. This would extend the capability of the Standard Model to describe the fundamental particles, thus it is essential that every part of the ILC be studied well to ensure that all events in the ILC are well understood. This study, through computer simulation using SimTools and ROOT programming, checks the capability of the Global Large Detector (GLD) calorimeter for the ILC in terms of response linearity and energy resolution. Using gamma and kaon0L as test particles, the energy response of the GLD calorimeter is determined to be linear as a function of incident energy. A calibration factor of 24.18 is obtained when using the energy deposit of gamma particles in the calorimeter. The energy resolution when using gamma particles is (14.92 ± 0.69)%/ $\sqrt{E}$ (1.9 ± 1.1)%, while for kaon0L particles is (45.98 ± 2.8)%/ $\sqrt{E}$ (11.3 ± 2.9)%. Varying the initial direction of particles does not affect the linearity of the energy response for both particles and on calculating the calibration factor when using gamma particles. It also reveals that the energy

resolution is better at the barrel region than at the endcap. From the analysis of the obtained data, we can conclude that the GLD calorimeter, in terms of response linearity and energy resolution, is a suitable calorimeter for the ILC project.

Keywords: collider, energy response linearity, energy resolution, calibration factor, barrel region, endcap region, calorimeter, gamma particles, kaon0L particles, Standard Model, SimTools, ROOT programming

CMPSD-58

STUDY OF AVALANCHE PROCESSES IN A GAS ELECTRON MULTIPLIER USING GARFIELD

Louie T. Murcia* and Hermogenes C. Gooc Jr.

Physics Department, MSU – Iligan Institute of Technology, Iligan City
E-mail: louie.murcia@physics.msuiit.edu.ph

A Time Projection Chamber (TPC) is the primary option for the main tracker of the detector at a future e^+e^- linear collider. The design issues for developing a high performance TPC are discussed with particular emphasis on the R&D, since using contemporary high-density readout electronics, a proportional gain of several thousand is required for fully efficient detection of minimum ionizing particle in thin layers of gas. A new type of gas amplification system, based on Gas Electron Multiplier (GEM) structures meets this challenge.

To study in details the operation mechanism of gas multiplication process and the charge transfer parameters in a GEM structure, the simulation program GARFIELD was used. First the field maps for the potential, electric field and dielectric medium were produced by MAXWELL using the method of finite elements. These files can be imported by GARFIELD and further drift simulations for the avalanche processes in a GEM can be run. The effective gain of the structure, defined as the ratio of collected to primary charge was measured by investigating the start and end points of the tracks followed by the created electrons and ions.

Results of the avalanche simulations worked at a mixture of 93%Argon-5%Isobutane-2%Carbon dioxide gas and performed at atmospheric and low pressure, with single electron starting from points randomly distributed above the GEM, give an effective gain from 10^4 up to 10^5. Half of the produced electrons are lost due to absorption on the lower surface of the GEM and approximately 40% of the total electrons can leave the GEM hole and a fraction of it contributes to the signal.

Keywords: Time Projection Chamber (TPC), Gas Electron Multiplier (GEM), GARFIELD, MAXWELL, avalanche process, effective gain.

CMPSD-59

GREEN FUNCTION AND ENERGY SPECTRUM OF A 3D DIRAC OSCILLATOR

Lyndon D. Bastatas and Jinky B. Bornales*

Physics Department, MSU – Iligan Institute of Technology
Email: ldbastatas@gmail.com, jbornales@yahoo.com

The Dirac oscillator is the counterpart of harmonic oscillator in relativistic quantum mechanics. It behaves like a harmonic oscillator with a spin-orbit coupling in the classical limit [Monshisky et al.,1989]. Here, we utilize the Feynman path integral prescription to obtain the Green function that satisfies the iterated Dirac equation for a three-dimensional Dirac oscillator.

The Green function, g(r'',r'), that satisfies the iterated Dirac equation is given by

$$\mathbf{g}(\mathbf{r}'',\mathbf{r}') = \frac{i}{2M}\sum_{s}\eta\eta^{*}\int_{0}^{\infty}\langle \mathbf{r}''|\exp\left\{-iH_{eff}\Lambda\right\}|\mathbf{r}'\rangle d\Lambda$$

where η=‹χ©m,› η*=‹m,©χ›,r=r(x,y,z) and $H_{eff} = M^2 - \hat{D}^2$ with

$\hat{D} = -\beta\,\boldsymbol{\alpha}\cdot\left(\mathbf{p} - iMf\,\beta\,\mathbf{r}\right) + \beta E$. Here α and β are the usual Dirac matrices, M is the mass of the particle, f is the oscillation frequency and E the energy and where and we set $\hbar = c = 1$.

The integrand in Eq.(1) is similar in form to a quantum propagator of a particle which starts at initial point $\mathbf{r}'$ and terminates at point $\mathbf{r}''$ that evolves in a time-like parameter Λ . Expressing the integrand as Feynman path integral, i.e.,

$$\langle x''y''z''|\exp\left\{-iH_{s}\Lambda\right\}|x''y''z''\rangle = \int\exp\left\{i\int_{0}^{\Lambda}L d\lambda\right\}d[xyz]$$

where L is the Lagrangian of the system. The Lagrangian can be obtained by performing the Legendre transformation which yields a form similar to a non-relativistic harmonic oscillator plus a term due to the spin-orbit coupling and some constants. The evaluation of the path integral, Eq.(2), is then carried by following the same procedure as in the non-relativistic case. Expressing the results in terms of Hermite polynomials, the second order Green function for the Dirac oscillator is

$$g(\mathbf{r}'',\mathbf{r}') = \sqrt{\frac{Mf^3}{\pi^3}} \sum_s \eta\eta^* \exp\left[\frac{-Mf}{2}\left\{(x'^2+x''^2)+(y'^2+y''^2)+(z'^2+z''^2)\right\}\right] \cdot$$

$$\sum_{l=0}^{\infty}\sum_{m=0}^{\infty}\sum_{n=0}^{\infty} \frac{1}{2^{l+m+n+1}(l!m!n!)} H_l\left(\sqrt{Mf}x'\right) H_l\left(\sqrt{Mf}x''\right) H_m\left(\sqrt{Mf}y'\right) H_m\left(\sqrt{Mf}y''\right)$$

$$\cdot H_n\left(\sqrt{Mf}z'\right) H_n\left(\sqrt{Mf}z''\right) \left\{ f\left(l+m+n+\frac{3}{2}\right)\left(\frac{f\beta}{2}+\frac{f\varepsilon}{2}(2j+1)+\frac{E^2-M^2}{2M}\right)-i\kappa \right\}^{-1}$$

in the limit as 0 where =± 1 and ε?=? 1.

The energy spectrum of the system can be extracted from the poles of Eq.(3). For positive energy states (when $\beta = +1$), $E^2 - M^2 = Mf\{2(N+1)+\varepsilon(2j+1)\}$

and for negative energy states (when $\beta = -1$), $E^2 - M^2 = Mf\{2(N+2)+\varepsilon(2j+1)\}$

where we set $N=l+m+n$ with $l,m,n = 0, 1, 2, \ldots$ These results agree to the spectrum obtained by Benitez et al. in 1990.

Keywords: relativistic quantum mechanics, Dirac oscillator, path integral, Green function, energy spectrum

CMPSD-60

ON THE PROPAGATOR OF A CHARGED PARTICLE IN A CONSTANT MAGNETIC FIELD WITH 2-D ANISOTROPIC HARMONIC OSCILLATOR POTENTIAL: A WHITE NOISE FUNCTIONAL APPROACH

Alviu Rey B. Nasir and Jinky B. Bornales

Department of Physics, MSU-Iligan Institute of Technology, Iligan City
Email: alviurey@gmail.com

The Feynman propagator for a charged particle in a constant magnetic field with a two-dimensional anisotropic harmonic oscillator potential is evaluated using white noise analysis. In this framework, the Feynman propagator can be expressed as,

$$K(x'',y'',z'';x',y',z';T) = \int I d\mu(\omega) \quad (1)$$

where $I = I_0 \delta(\mathbf{x}(T)-\mathbf{x}') \exp\left[-i\int_0^T V(\mathbf{x}(\tau))d\tau\right]$ and

$I_0 = N \exp\left[\left(\frac{i+1}{2}\right)\int_0^T \omega(\tau)^2 d\tau\right]$. For the system being considered, the potential V is given by $V = \Omega_y^2 y^2 + \Omega_z^2 z^2 - \gamma(x\dot{y} - y\dot{x})$. In white noise analysis, the integration over the Gaussian white noise measure $d\mu(\omega)$ in Eq. (1) is just the T-transform of the functional I. Performing the T-transform and following the procedures discussed separately in a paper by C.C. Bernido and M.V. Carpio-Bernido (2002) and in a paper by de Faria et al. (1991), we obtained the following results:

$$K(x'', y'', z''; x', y', z'; T)$$

$$= [H(\Omega)]^{-1/2} K_0(x'', x'; T) K_{\Omega_y}(y'', y'; T) K_{\Omega_z}(z'', z'; T) \exp\left[\frac{i\gamma}{2}(x''y'' - x'y')\right]$$

$$\times \exp\left[\frac{i\gamma^2 g(\Omega T)}{2\Omega^3 T^2 H(\Omega T)}(x'-x'')^2 + \frac{i\gamma \tan\frac{\Omega T}{2}}{\Omega T H(\Omega T)}(x'-x'')(y'+y'') + \frac{i\gamma \tan^2\frac{\Omega T}{2}}{2\Omega^2 T H(\Omega T)}(y'+y'')^2\right]$$

where, $K_0(x'', x'; T)$, $K_{\Omega_y}(y'', y'; T)$, and $K_{\Omega_z}(z'', z'; T)$ are propagators for free-particle in x, harmonic oscillator in z, respectively; $\gamma = qH$, q is the charge, H is the magnetic field; $\Omega^2 = \Omega_y^2 + \gamma^2$, Ω_y is the frequency along y; $H(\Omega T) = 1 - \gamma^2 g(\Omega T)/(\Omega^3 T)$, $g(\Omega T) = \Omega T - 2\tan(\Omega T/2)$. The final propagator agrees with the known result.

Keywords: Brownian motion, white noise analysis, T-transform, Feynman path integral, functional

CMPSD-61

WHITE NOISE APPROACH ON THREE DIMENSIONAL ANISOTROPIC HARMONIC OSCILLATOR IN A MAGNETIC FIELD

Norhabib P. Paporo, Jingle B. Magallanes* and Jinky B. Bornales

Theory Group, Department of Physics, Mindanao State University - Iligan Institute of Technology (MSU-IIT), 9200 Iligan City
Email: jbmagallanes@gmail.com

The two and three-dimensional anisotropic harmonic oscillator (AHO), which describes the behavior of the electron in an anisotropic lattice in semiconductor physics, have been solved successfully through Feynman Calculus or time-slicing method. In this study, the 3-dimensional AHO in a magnetic field is resolved via a different approach called the white noise functional, which is mathematically well established compared to the time-slicing method. Although Feynman calculus had penetrated the problems in quantum mechanics with great success but it lacks the solid mathematical foundation. In the white noise approach, the effective action of AHO with external magnetic field is set-up and expressed in terms of the white noise variable $\omega(\tau)$, or just the time derivative of the Brownian motion, and following the procedures discussed in the separate papers of B.K. Cheng (J. Phys. A: Math. Gen. 17, 1984) and C.C. Bernido, et al. (Functional Integrals in Stochastic and Quantum Dynamics, Jagna, Bohol, CVIF, 2001), the propagator separable in xy and z resulted. Finally, employing the change of coordinates from Cartesian to Cylindrical system, the propagator for AHO is obtained as expressed in the paper of D. Peak, et al. (Journal of Mathematical Physics, Volume 10, Number 8, August 1969) which was done through the method of time-slicing.

Keywords: white noise functional, time-slicing method, anisotropic harmonic oscillator, brownian motion

CMPSD-62

INVESTIGATION ON THE DIFFERENCE BETWEEN THE SOUND EMITTED BY QUEEN-RIGHT AND QUEENLESS HIVES OF TRIGONA BIROI

Francis Murillo Emralino*[1], Marvin Ustaris Herrera[1], Cleofas Cervancia[2]
francis_emralino@yahoo.com, muherrera@yahoo.com, dorsata1@yahoo.com

[1]Physics Division, Institute of Mathematical Sciences and Physics
University of the Philippines - Los Baños
C-203 Physical Sciences Building, UPLB, College, Laguna 4031
Tel.: (049) 536-1841; Fax: (049) 536-6610
[2]Institute of Biological Sciences
University of the Philippines - Los Baños
Biological Sciences Building, UPLB, College, Laguna 4031

Investigations on the frequency of the sounds produced by the stingless bee Trigona biroi were done. This is to determine the possible frequency range difference that would arise between a queen-right hive and a queenless hive. Frequency analysis showed the presence of an additional frequency peak in the absence of the queen.

We sampled three hives and recorded the sound coming from each one with the use of Logger Pro™ Microphone. Sound recordings were done at 5- and 10-second durations, 10 trials for each. A hive was then intentionally divided to insure the absence of the queen and the same recording procedures were done. The raw data (sound pressure versus time) was obtained through the use of LabPro™ interface and stored on the computer.

In order for us to determine the frequency of the sounds of these bees, Fast Fourier Transforms (FFT) was applied to the data gathered which was projected as a graph of amplitude versus frequency. The resulting FFT graphs revealed frequency peaks at 300-350 Hertz and this was generally observed for each of the recordings that were done in all hives. It is also important to note the presence of a peak at 200 Hertz which was gradually reduced as recordings proceeded.

Upon the division of one of the hives however, in which case the hive is already queenless, we observed an additional peak at 200 Hertz and considerably higher than the 300-350 Hertz peak that was observed when the colony was still intact. This observed peak on the queenless colonies could indicate when the queen is present or not in a hive.

Keywords: stingless bees, trigona biroi, fast fourier transforms, frequency peaks